

ARTICLE TYPE

Gaia search for stellar companions of TESS Objects of Interest V

Markus Mugrauer | Ann-Kathrin Kollak | Lara Pietsch | Kai-Uwe Michel

Astrophysikalisches Institut und
Universitäts-Sternwarte Jena

Correspondence

M. Mugrauer, Astrophysikalisches Institut
und Universitäts-Sternwarte Jena,
Schillergäßchen 2, D-07745 Jena, Germany.
Email: markus@astro.uni-jena.de

In this paper we present the latest results of our ongoing multiplicity survey of (Community) TESS Objects of Interest, using astrometry and photometry from the latest data release of the ESA Gaia mission to detect stellar companions of these stars and to characterize their properties. A total of 92 binary and two hierarchical triple star systems are identified among the 745 target stars whose multiplicity is explored in this study, all at distances of less than 500 pc around the Sun. As expected for components of gravitationally bound star systems, the targets and the detected companions are at the same distance and share a common proper motion, as shown by their accurate Gaia astrometry. The companions have masses of about 0.12 to $1.6 M_{\odot}$ and are most frequently found in the mass range up to $0.6 M_{\odot}$. The companions have projected separations from the targets between about 110 and 9600 au. Their frequency is highest and constant from about 300 to 800 au, decreasing at larger projected separations. In addition to main sequence stars, five white dwarf companions are detected in this study, whose true nature is unveiled by their photometric properties.

KEYWORDS:

binaries: visual, white dwarfs,

stars: individual (TOI 5389 B, TOI 5628 B, CTOI 29106627 B, CTOI 320261550 B, CTOI 333792947 B)

1 | INTRODUCTION

In the course of our ongoing multiplicity survey of (Community) TESS¹ Objects of Interest ((C)TOIs) stellar companions of these stars are detected and their properties are characterized using astrometric and photometric data, originally taken from the 2nd and early 3rd data releases (Gaia Collaboration et al., 2018, 2021), and finally from the full 3rd data release (Gaia DR3 from hereon, Gaia Collaboration et al., 2023) of the European Space Agency (ESA) Gaia mission. The first results of the survey have already been published in Mugrauer and Michel (2020), Mugrauer and Michel (2021), Mugrauer, Zander, and Michel (2022), and Mugrauer, Rück, and Michel (2023). Further information on the survey is summarized in these publications. Since then, many of these (C)TOIs, which were found to be members of multiple star systems in our survey, have been confirmed as exoplanet host stars

by follow-up observations, for example: TOI 128, TOI 199, TOI 444, TOI 470, TOI 762, TOI 815, TOI 837, TOI 858, TOI 880, TOI 907, TOI 1052, TOI 1248, TOI 1450, TOI 1473, TOI 1824, TOI 1855, TOI 1859, and TOI 1937, which are listed in the Extrasolar Planets Encyclopaedia² (see Schneider, Dedieu, Le Sidaner, Savalle, & Zolotukhin, 2011, and references therein). The targets of our survey are all listed in the (C)TOI release of the Exoplanet Follow-up Observing Program for TESS³ (ExoFOP-TESS).

In this paper we investigate the multiplicity status of more than 700 (C)TOIs listed in the ExoFOP-TESS, that have not yet been studied in our survey, using data from the Gaia DR3. The following section describes in detail the properties of the selected targets and the search for companions around these stars. Section 3 presents all (C)TOIs with detected companions

²Online available at: <https://exoplanet.eu/>.³Online available at:https://exofop.ipac.caltech.edu/tess/view_toi.php
https://exofop.ipac.caltech.edu/tess/view_ctoi.php.¹TESS: Transiting Exoplanet Survey Satellite (Ricker et al., 2015).

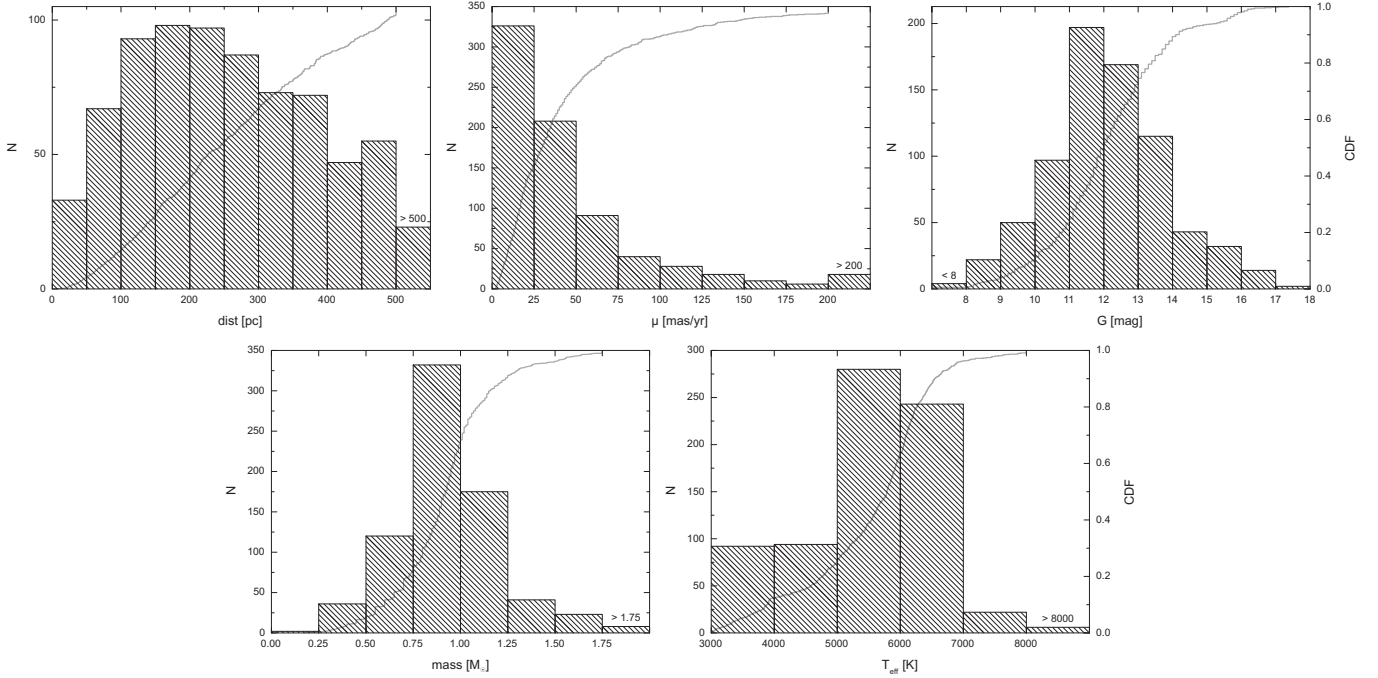


FIGURE 1 The histograms and CDFs of the individual properties of the targets, whose multiplicity is investigated in this study. The histograms and CDFs of the distance $dist$, total proper motion μ , and G-band magnitude are based on the Gaia DR3 data of all 745 targets. Masses and T_{eff} of the targets are taken from the SHC or SHC2 where available, which is the case for 737 targets.

and discusses the properties of these star systems. Finally, the last section summarizes the current status of our survey and provides an outlook on the project.

2 | SEARCH FOR STELLAR COMPANIONS OF (C)TOIS BY EXPLORING THE GAIA DR3

In our study, stellar companions of the investigated (C)TOIs are firstly identified as sources that are located at the same distance as the targets and secondly share a common proper motion with these stars. In order to unambiguously detect co-moving companions and confirm their equidistance to the (C)TOIs, we consider in our study only those sources for which a significant measurement of their parallax ($\pi/\sigma(\pi) > 3$) and proper motion ($\mu/\sigma(\mu) > 3$) is available in the Gaia DR3. Sources with a negative parallax are not taken into account.

In this paper, we explore the multiplicity of 745 (C)TOIs that have not yet been investigated in the course of our survey with Gaia DR3 data, that meet the distance constraint of our survey, described in Mugrauer (2019) or Mugrauer and Michel (2020), and are therefore selected as targets for this study. Figure 1 shows the histograms and the cumulative distribution functions (CDFs) of the individual properties of these stars. The distance ($dist$) and total proper motion (μ) of all targets are determined

using their precise Gaia DR3 parallax and proper motion in right ascension and declination. The G-band magnitude of all targets is listed in the Gaia DR3, while their mass and effective temperature (T_{eff}) are taken from the Starhorse catalog (SHC from here on, Anders et al., 2019) or from the Starhorse 2 catalog (SHC2 from here on, Anders et al., 2022) where available, which is the case for 737 stars, that is, the vast majority ($\sim 99\%$) of all targets. The targets have distances from the Sun between about 7 and 800 pc, proper motions in the range between about 1 and 840 mas/yr, G-band magnitudes between 6.3 and 17.4 mag, masses between about 0.18 and $4.4 M_{\odot}$, and T_{eff} between about 3000 and 12000 K. According to the CDFs of the individual properties, the targets are most commonly located at distances between about 50 and 400 pc, have typical proper motions from about 4 to 24 mas/yr, and G-band magnitudes from about $G = 11$ to 13 mag. The targets are mainly solar-like stars with masses between about 0.8 and $1.2 M_{\odot}$. This population is also recognizable in the T_{eff} -distribution of the targets at intermediate temperatures from about 4700 to 6300 K.

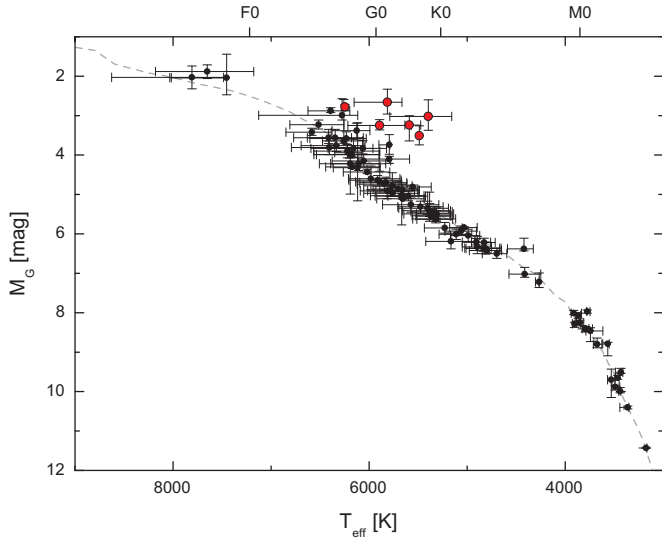


FIGURE 2 The absolute G-band magnitude M_G plotted versus the T_{eff} of all (C)TOIs with detected companions, which are presented here. (C)TOIs listed in the SHC or if not available there in the SHC2 with surface gravities $\log(g[\text{cm/s}^2]) < 4.0$ are shown as red circles, those with larger surface gravities as black circles, respectively. The main sequence from Pecaut and Mamajek (2013) is drawn as a grey dashed line for comparison.

As described in Mugrauer (2019) or Mugrauer and Michel (2020), our survey is restricted to companions with projected separations of up to 10000 au. With π the Gaia DR3 parallax of the (C)TOIs this results in an angular search radius for companions around the targets:

$$r[\text{arcsec}] = 10\pi[\text{mas}] \quad (1)$$

All sources listed in the Gaia DR3 that are located within the search radius used around the targets and have a significant parallax and proper motion are considered as companion-candidates. A total of about 7749 such objects are detected around 745 targets, and their multiplicity is explored in the study, presented here. The companionship of all these candidates is examined using their precise Gaia DR3 astrometry and that of the associated (C)TOIs, following exactly the procedure, which is described in Mugrauer (2019) or Mugrauer and Michel (2020). The vast majority of these sources can be excluded as companions because they and the associated (C)TOIs do not share a common proper motion and/or are not located at the same distance as these stars. In contrast, 96 candidates can be confidently identified as companions of the (C)TOIs based on their accurate Gaia DR3 astrometry. The properties of these companions and the associated (C)TOIs are described in detail in the next section of this paper.

3 | (C)TOIS AND THEIR DETECTED STELLAR COMPANIONS

The mass, T_{eff} , and absolute G-band magnitude of all the (C)TOIs with detected companions, presented here, are listed in the SHC or SHC2. We plot these stars in a $T_{\text{eff}}-M_G$ -diagram in Figure 2 with the main sequence from Pecaut and Mamajek (2013)⁴ for comparison. While most targets with detected companions are main sequence stars a few (C)TOIs are (significantly) located above the main sequence. These stars also have a surface gravity of $\log(g[\text{cm/s}^2]) < 4$, as listed in the SHC or, if not available there, in the SHC2, and are therefore classified as (sub)giant stars.

The parallax, proper motion, apparent G-band magnitude, and extinction estimate (A_G) of the (C)TOIs and their companions detected in this study are summarized in Table 3, which lists a total of 92 binary, and two hierarchical triple star systems.

With the accurate Gaia DR3 astrometry we determine the angular separation (ρ) and position angle (PA) of all detected companions to the associated (C)TOIs. The derived relative astrometry of the companions is summarized in Table 4. Its uncertainty remains below about 0.9 mas in angular separation and 0.02° in position angle.

Table 4 also lists the parallax difference $\Delta\pi$ between the (C)TOIs and their companions, together with its significance $\text{sig-}\Delta\pi$, which is also calculated taking into account the astrometric excess noise of each object. The same table contains for each companion its differential proper motion μ_{rel} relative to the associated (C)TOI with its significance, and its common proper motion (cpm) index. The cpm -index, as defined in Mugrauer (2019) or Mugrauer and Michel (2020), characterizes the degree of common proper motion of a detected companion with the associated (C)TOI:

$$cpm\text{-index} = |\vec{\mu}_{(C)TOI} + \vec{\mu}_{Comp}|/\mu_{\text{rel}} \quad (2)$$

with $\vec{\mu}_{(C)TOI}$ the proper motion of the (C)TOI, and $\vec{\mu}_{Comp}$ the proper motion of the companion, as well as its differential proper motion $\mu_{\text{rel}} = |\vec{\mu}_{(C)TOI} - \vec{\mu}_{Comp}|$.

The parallaxes of the individual components of the star systems, detected in this study, do not differ significantly from each other ($\text{sig-}\Delta\pi < 3$) when the astrometric excess noise is considered. This clearly proves the equidistance of the detected companions and the (C)TOIs, as expected for components of physically associated star systems. All of the detected companions have a $cpm\text{-index} \geq 10$, that is, the detected companions and the associated (C)TOIs clearly form common

⁴Online available at: https://www.pas.rochester.edu/~emamajek/EEM_dwarf_UBVIJHK_colors_Teff.txt. The version used here is 2022.04.16.

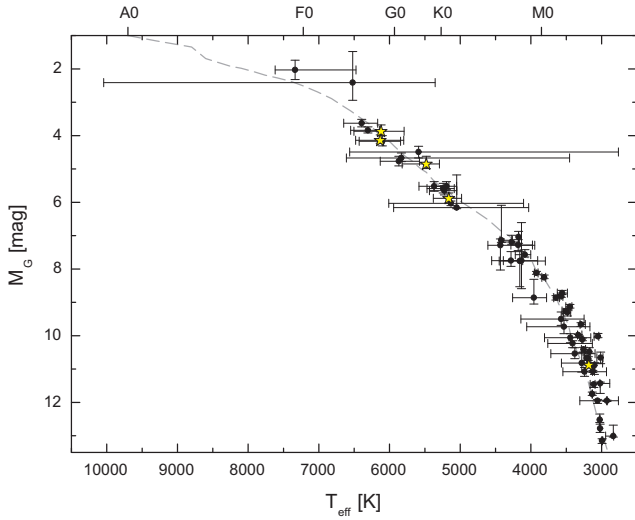


FIGURE 3 The absolute G-band magnitude M_G plotted over the T_{eff} of all detected companions whose T_{eff} are listed in either the SHC or SHC2, or for which Apsis GSP-Phot Aeneas temperature estimates are available. Companions, which are the primary components in their star system, are shown as yellow star symbols. The main sequence from Pecaut and Mamajek (2013) is drawn as a dashed grey line for comparison.

proper motion pairs, as expected for gravitationally bound star systems.

The absolute G-band magnitude of all detected companions is taken from the SHC or, if not available there, from the SHC2, indicated by the SHC2 flag in Table 5. Where the absolute magnitude of the companions is not listed in these catalogs, it is inferred from their apparent G-band photometry and the parallax of the (C)TOIs, and the SHC (if available) or the SHC2 G-band extinction estimate, otherwise the A_G estimate from Vizier. The extinction estimate of the companions is used if available, otherwise that of the (C)TOIs, as indicated in Table 3. In general, the used A_G estimates are in good agreement with those determined by other authors, as listed in the Vizier database, or those derived from dust infrared emission maps (see e.g., Schlafly & Finkbeiner, 2011; Schlegel, Finkbeiner, & Davis, 1998). The deviation of the individual A_G estimates is on average 0.16 mag, which, as expected, matches the mean uncertainty of the used extinction estimates. In this context, it should be emphasized that the derived absolute magnitude of the companions and thus also their mass and T_{eff} also depend on the used extinction estimate. If this estimate is set too high/low, the derived mass and T_{eff} of the companions are also higher/lower. For the typical companions detected in this study (average mass of about $0.5 M_\odot$), a deviation in A_G of 0.16 mag leads to a mass shift of about $0.03 M_\odot$ and about 50 K in T_{eff} , which is smaller than the mean uncertainty of both quantities (about $0.05 M_\odot$, and 200 K), as listed in Table 5.

The projected separation of all companions is determined from their angular separation from the associated (C)TOI and the parallax of these stars.

The mass and T_{eff} of the companions presented here, including their uncertainties, are from the SHC or the SHC2 (indicated by the SHC2 flag in Table 5) where available, which is the case for about 63 % of all detected companions. We plot these companions in Figure 3 in a $T_{\text{eff}}-M_G$ -diagram together with those companions for which an estimate of their T_{eff} is determined by Apsis GSP-Phot⁵ using the MCMC algorithm Aeneas⁶, as indicated by the AEN flag in Table 5. As illustrated in Figure 3, the absolute photometry and T_{eff} of all these companions are in good agreement with those expected for main sequence stars.

For the remaining 36 companions their mass and T_{eff} are determined from their absolute G-band magnitude via interpolation (inter flag in Table 5) using the M_G -mass- and M_G-T_{eff} -relation from Pecaut and Mamajek (2013), assuming that these companions are main sequence stars. In order to test this hypothesis, we compare the obtained T_{eff} of the companions either with their Apsis GSP-Phot Aeneas temperature estimate, if available, or with the T_{eff} of the companions obtained from their $(B_p - R_p)$ color and reddening estimate $E(B_p - R_p)$ ⁷, using the $(B_p - R_p)_0-T_{\text{eff}}$ -relation from Pecaut and Mamajek (2013).

For all but five of these companions, their T_{eff} , determined from their absolute G-band magnitude and assuming that they are main sequence stars, agrees well with their Apsis GSP-Phot Aeneas temperature estimate or with the temperature derived from their color. The typical deviation of the different temperature estimates is about 390 K, which is consistent with the precision of the derived T_{eff} . We therefore conclude that all of these companions are main sequence stars.

In addition, we also compare the Gaia DR3 $(B_p - R_p)$ color of the (C)TOIs and their companions (if any), indicated by the BPRP flag in Table 5. For main sequence stars, companions fainter/brighter than the (C)TOIs are expected to appear redder/bluer than the stars, and this is true for most of the discovered companions, with the exception of TOI 5389 B, TOI 5628 B, CTOI 29106627 B, and CTOI 320261550 B. Three of these four companions were also observed with the Panoramic Survey Telescope and Rapid Response System (Pan-STARRS) and their color composite images are shown in Figure 4. In these images, the faint companions are clearly visible as bluish sources next to the

⁵The General Stellar Parametrizer from Photometry (GSP-Phot) is one of the major component modules in the astrophysical parameters inference system (Apsis) of Gaia.

⁶GSP-Phot Aeneas estimates the T_{eff} of detected sources from their low-resolution BP/RP spectra, apparent G-band magnitude and parallax.

⁷The reddening of an object is estimated from its extinction A_G , using the relation $A_G/E(B_p - R_p) = 1.890 \pm 0.015$ from Wang and Chen (2019).

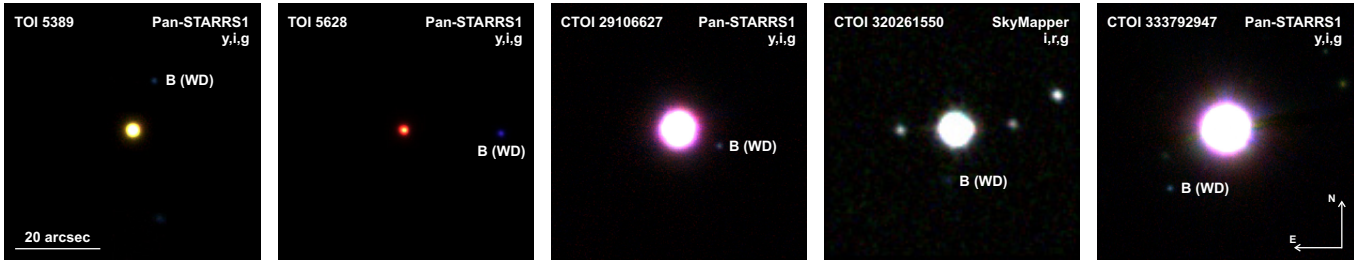


FIGURE 4 (RGB)-color images of TOI 5389, TOI 5628, CTOI 29106627, and CTOI 333792947 with their white dwarf companions composed of y-, i- and g-band Pan-STARRS images. The image of CTOI 320261550 and its white dwarf companion is made of i-, r-, and g-band images taken in the SkyMapper Southern Sky Survey.

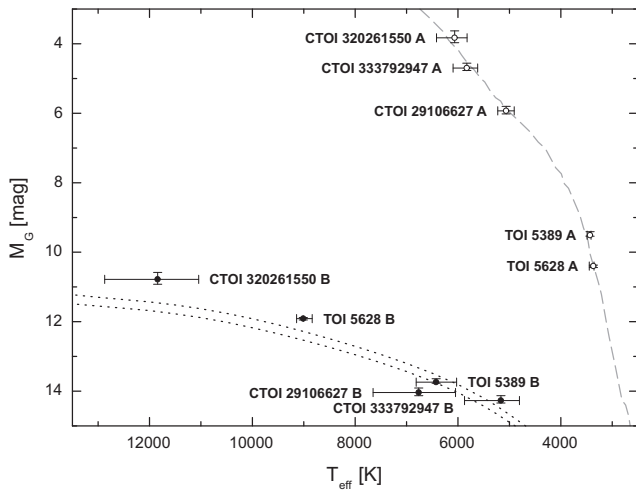


FIGURE 5 The absolute magnitude M_G plotted against the T_{eff} of the components of all star systems with detected white dwarf companions. The grey dashed line shows the main sequence, the black dotted lines the evolutionary mass tracks of DA white dwarfs with masses of 0.5 and $0.6 M_{\odot}$. The primaries of the systems are shown as white circles, the white dwarf secondaries as black circles, respectively.

associated much brighter (C)TOIs. The same applies to the faint companion CTOI 320261550 B, imaged as part of the SkyMapper Southern Sky Survey. The color composite image of this companion is also shown in Figure 4.

The photometric properties of all these companions are summarized in Table 1. The companions are several magnitudes fainter than the (C)TOIs, but appear bluer than these stars. The temperatures of the companions derived from their colors are significantly higher (by about 3600 to 8600 K) than the temperatures, derived from their absolute magnitudes in the G-band, assuming that they are main sequence stars.

These companions, along with the other components of their star system, are plotted in a M_G - T_{eff} -diagram in Figure 5. The main sequence from Pecaut and Mamajek (2013) and the mass

tracks from the Bergeron et al. evolutionary models⁸ are plotted in this diagram for comparison. While the brighter primary components of these systems are main sequence stars, the faint secondary stars are all located well below the main sequence, and their Gaia photometry is the most consistent with that expected for white dwarfs. We therefore conclude that these companions are white dwarfs, as indicated by the WD flag in Table 5.

Another white dwarf, CTOI 333792947 B, which is also shown in Figure 5, is revealed in this study because of its comparable color ($\Delta(B_p - R_p) = 0.229 \pm 0.205$) but large magnitude difference to its primary star ($\Delta G \sim 9.6$ mag).

Figure 6 shows the histograms and CDFs of the properties of all the companions detected in this study. The companions have angular separations from the (C)TOIs ranging from about 0.8 to 111 arcsec, corresponding to projected separations of 113 to 9611 au. According to the underlying CDF, the frequency of companions is highest and constant between about 300 and 800 au, and decreases at larger projected separations. Half of all companions have projected separations of less than 1300 au. A total of three stellar systems with projected separations below 200 au are detected, namely: TOI 5319 AB, CTOI 199572211 AB, CTOI 287643871 AB, that is, these systems are the most challenging environments for planet formation identified in this study.

The companion masses range from about 0.12 to $1.6 M_{\odot}$ (average mass: $\sim 0.5 M_{\odot}$). The highest companion frequency in the CDF is found in the mass range up to $0.6 M_{\odot}$, corresponding to mid-M to late-K dwarfs, according to the relation between mass and spectral type (SpT) from Pecaut and Mamajek (2013). At higher masses, the companion frequency decreases continuously towards higher masses. This peak in the companion population is also present in the distribution of

⁸The models are available online at: <https://www.astro.umontreal.ca/~bergeron/CoolingModels/>. The version used here is 2021.01.13. For more details about the models, see: Bédard, Bergeron, Brassard, & Fontaine, 2020; Bergeron et al., 2011; Blouin, Dufour, & Allard, 2018; Holberg & Bergeron, 2006; Kowalski & Saumon, 2006; Tremblay, Bergeron, & Gianninas, 2011.

TABLE 1 In this table we summarize the photometric properties of all the white dwarf companions, detected in this study. For each companion we list the color difference $\Delta(B_p - R_p)$ and the G-band magnitude difference ΔG to the associated (C)TOI, its apparent $(B_p - R_p)$ color, as well as its derived intrinsic color $(B_p - R_p)_0$ and T_{eff} .

Companion	ΔG [mag]	$\Delta(B_p - R_p)$ [mag]	$(B_p - R_p)$ [mag]	$(B_p - R_p)_0$ [mag]	T_{eff} [K]
TOI 5389 B	4.266 ± 0.007	-1.718 ± 0.118	0.622 ± 0.118	$0.620^{+0.118}_{-0.128}$	6425^{+389}_{-399}
TOI 5628 B	1.625 ± 0.004	-2.582 ± 0.014	0.079 ± 0.011	$0.042^{+0.022}_{-0.016}$	9008^{+131}_{-173}
CTOI 29106627 B	8.137 ± 0.007	-0.551 ± 0.203	0.559 ± 0.203	$0.513^{+0.208}_{-0.213}$	6764^{+888}_{-716}
CTOI 320261550 B	7.223 ± 0.004	-0.926 ± 0.062	-0.117 ± 0.062	$-0.245^{+0.088}_{-0.113}$	11841^{+1031}_{-797}
CTOI 333792947 B	9.578 ± 0.007	0.229 ± 0.205	1.052 ± 0.205	$1.017^{+0.208}_{-0.217}$	5165^{+708}_{-361}

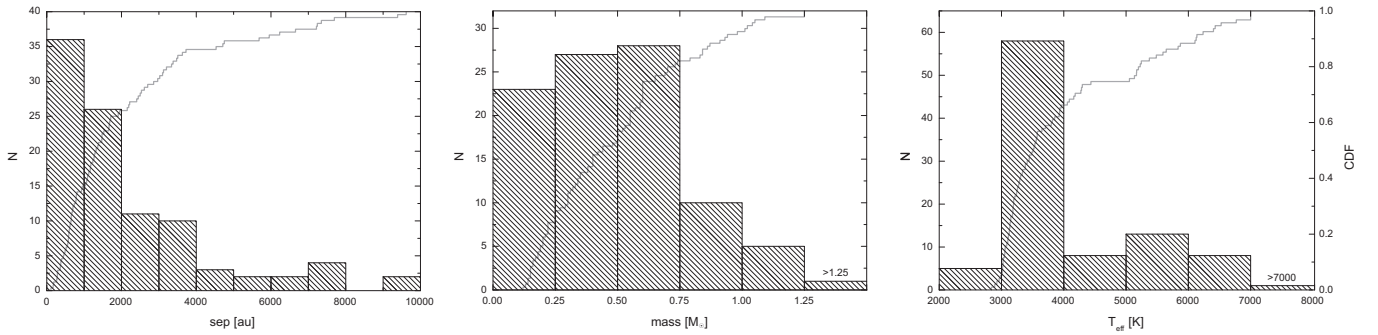


FIGURE 6 The histograms and CDFs of the projected separation, mass, and T_{eff} of all detected companions, presented here.

their T_{eff} , where the companion frequency is highest at temperatures between about 3000 and 4000 K. As can be seen from the separation-mass diagram in Figure 7, of the 96 companions presented here, five are the primary, 89 the secondary and two the tertiary components of their star system.

In order to characterize the detection limit, achieved in this study, we plot the magnitude difference of all detected companions over their angular separation from the associated (C)TOIs, as shown in Figure 8. For comparison, we show the Gaia detection limit, determined by Mugrauer et al. (2023). As expected, all detected companions, presented here, remain within this limit.

The magnitude difference expected between the targets of this study and low-mass main sequence companions (shown as grey dashed lines in Figure 8) is estimated using the expected absolute G-band magnitude of these stars, as listed in Pecaut and Mamajek (2013), and the average of the absolute G-band magnitude of our targets ($M_G \sim 5.0$ mag). As can be seen in Figure 8, a magnitude difference of about 4 mag is achieved at an angular separation of about 0.9 arcsec around the targets of this study. This allows the detection of companions with masses down to about $0.5 M_\odot$ (the average mass of all companions detected) separated from the (C)TOIs by more than 230 au. In addition, all stellar companions with masses above

$0.1 M_\odot$ are detectable beyond ~ 3 arcsec, which corresponds to a projected separation of about 770 au at the average target distance of 255 pc.

4 | SUMMARY AND OUTLOOK

Several ground-based either Seeing limited or high contrast imaging surveys have been performed in the past to study the multiplicity of exoplanet host stars, among others, for example, Mugrauer, Ginski, and Seeliger (2014), or Mugrauer and Ginski (2015), and Ginski et al. (2016). Here we present the latest results of our survey using data from ESA's Gaia mission, which is based on methods first applied on Gaia data in the multiplicity survey of exoplanet host stars, performed by Mugrauer (2019). Later, other comprehensive stellar multiplicity surveys were also carried out using Gaia data (see e.g. El-Badry, Rix, & Heintz, 2021; Kervella, Arenou, & Thévenin, 2022).

In the present study, we use Gaia DR3 data to search for stellar companions of 745 (C)TOIs announced in the (C)TOI release of the ExoFOP-TESS and whose multiplicity has not yet been explored in the course of our survey. A total of 7749 sources were detected around 567 targets with accurate

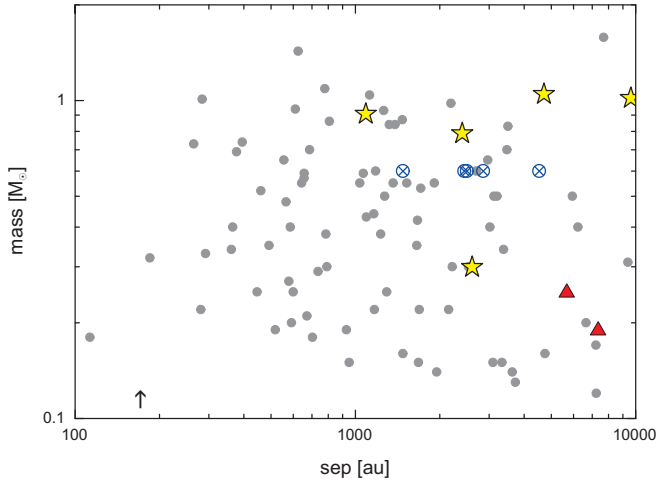


FIGURE 7 The mass of all detected companions, presented here, plotted over their projected separation. Companions that are the primary component of their star system are shown as yellow star symbols, secondaries as grey circles, and tertiary components as red triangles, respectively. Detected white dwarf companions, for which a mass of $0.6 M_{\odot}$ is assumed, are plotted as blue crossed circles. Note that the symbols of the white dwarf companions TOI 5389 B, and TOI 5628 B overlap at a separation of about 2500 au. The separation of the companion CTOI 287643871 B, for which no mass could be determined because its G-band magnitude is not listed in the Gaia DR3, is marked by a black arrow.

astrometric solutions in the Gaia DR3, while no companion-candidates were found around the remaining 178 targets of this study within the applied search radius. In total, new co-moving companions were detected around 94 of all targets whose multiplicity is studied here. In addition, companions around another 20 (C)TOIs were found in the Gaia DR3, but were already identified in the Gaia DR2 by Mugrauer (2019) and Mugrauer and Michel (2020) or most recently by Michel and Mugrauer (2024), who used Gaia DR3 data to study the multiplicity of confirmed exoplanet host stars. The multiplicity rate of the examined (C)TOIs is thus at least $15.3 \pm 1.4\%$, which agrees well with the (C)TOI multiplicity rate of $14.9 \pm 1.1\%$, recently reported by Mugrauer et al. (2023).

Color-composite images of some of the detected star systems are shown in Figure 9, taken with the Cassegrain-Teleskop-Kamera-II (CTK-II from hereon, Mugrauer, 2016) at the University Observatory Jena. In addition to 92 double stars, two hierarchical triple star systems are detected in which the (C)TOIs have both a close and a distant stellar companion. In addition, an astrometric non-single star solution for the co-moving companion TOI 4660 B is listed in the Gaia DR3

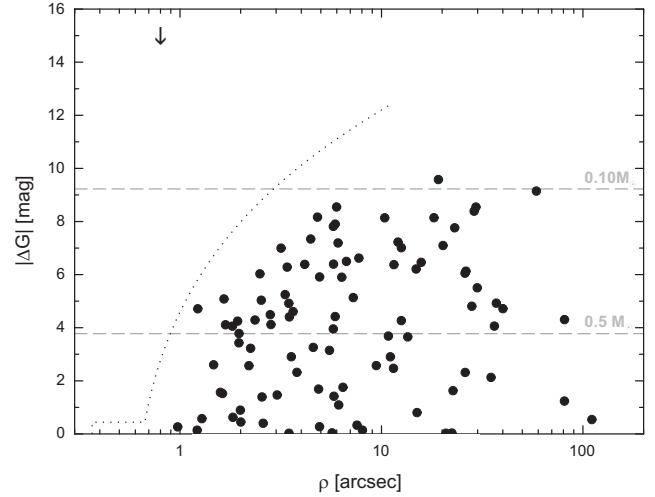


FIGURE 8 The G-band magnitude difference $|\Delta G|$ of all detected companions, presented here, plotted versus their angular separation ρ from the associated (C)TOIs. The Gaia detection limit, determined by Mugrauer et al. (2023), is drawn as a dotted line for comparison. The grey dashed horizontal lines show the expected average magnitude differences for companions of $0.1 M_{\odot}$ and $0.5 M_{\odot}$, respectively. The angular separation of the companion CTOI 287643871 B, for which no G-band magnitude is listed in the Gaia DR3, is indicated by a black arrow.

(marked with the flag NSS in Table 5). Based on 230 astrometric measurements made with Gaia for this star, a significant ($\text{sig} > 30$) time-varying acceleration ($\dot{\mu} = 2.75 \pm 0.13 \text{ mas/yr}^2$ and $\ddot{\mu} = 17.85 \pm 0.51 \text{ mas/yr}^3$) of the companion in the plane of the sky is detected, indicating that it is itself a close binary system. The orbital period of this system must be significantly longer than the 34-month period on which the Gaia DR3 is based. We therefore classify TOI 4660 as a potential hierarchical triple star system, whose triple nature needs to be confirmed by follow-up observations.

The Washington Double Star catalog (WDS from hereon, Mason, Wycoff, Hartkopf, Douglass, & Worley, 2001), which is available in the VizieR database, list 18 of the companions identified in this study either as co-moving companions or as companion-candidates of the (C)TOIs, so confirmation of their companionship is required, which is finally provided by this study. Although the WDS is currently the most complete catalogue of multiple star systems available, containing relative astrometric measurements of multiple star systems over a period of more than 300 years, 78 (i.e., about 81 % of all) companions, detected in this study, are not listed in the WDS and marked with the \star flag in the Table 4. Additional companions that are not included in the WDS because they were

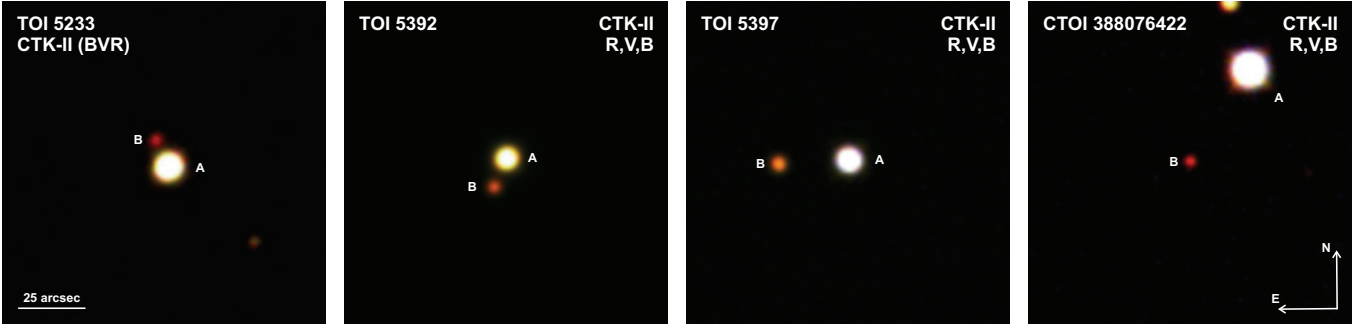


FIGURE 9 (RGB)-color images of the binary systems TOI 5233 AB, TOI 5392 AB, TOI 5397 AB, and CTOI 388076422 BA, composed of R-, V-, and B-band images, taken with the CTK-II at the University Observatory Jena.

detected in the Gaia data releases are listed in the WDS Supplemental Catalogue (WDSS), which is not included in the VizieR database but is available for download in its latest version⁹. Companions detected in this survey that are listed neither in the WDS nor WDSS are indicated with the $\star\star$ flag in Table 4. This shows the great potential of the ESA Gaia mission for stellar multiplicity surveys, especially for the detection of stellar companions on wide orbits, as shown by the derived detection limit of this study in Figure 8. On average, all stellar companions with masses above about $0.1 M_{\odot}$ are detectable around the targets of this study at angular separations larger than about 3 arcsec (or 770 au of projected separation), and about 68 % of all detected companions have such separations. At the average distance of our targets of 255 pc, this mass limit also corresponds to the faintest detectable companions ($G = 21$ mag), which exhibit significant measurements of parallax ($\pi/\sigma(\pi) > 3$) and proper motion ($\mu/\sigma(\mu) > 3$) in the Gaia DR3. Overall, companions are detected at projected separations between about 110 and 9600 au, and the companion frequency is highest at separations between about 300 and 800 au, decreasing significantly at larger projected separations.

The apparent lack of close companions with projected separations below 300 au is due to the Gaia detection limit, as illustrated in Figure 8, according to which the direct detection of low-mass stellar companions in particular is only possible with Gaia at projected separations beyond a few hundred au. This also becomes clear when comparing the CDF of the projected separation of all companions detected in this study with that of companions of solar like stars (the typical targets of our survey) as determined by Raghavan et al. (2010), both of which are shown in Figure 10.

Within the projected separation range considered here (100–10000 au), the CDFs are significantly different from each other ($D_{\max} = 0.338$ at ~ 550 au \rightarrow KS-Test: $\alpha < 10^{-9}$). The lack

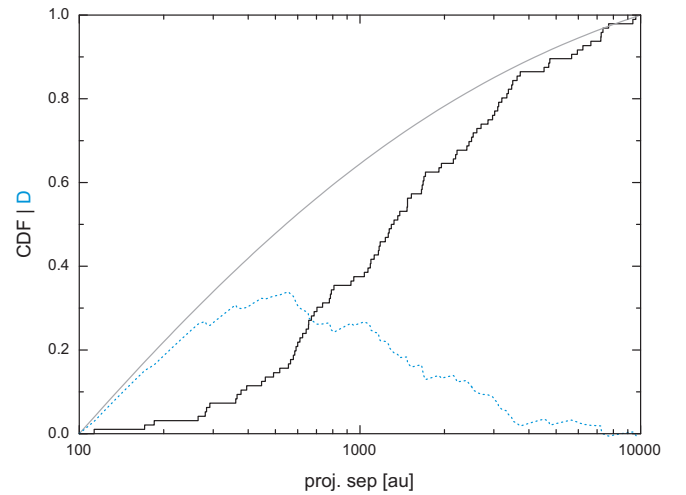


FIGURE 10 The CDF of the projected separation of all companions, detected in this study (black line), and that of stellar companions of solar type stars (grey line) for the range of projected separation between 100 and 10000 au. The discrepancy between both CDFs is shown as blue line. The increasing discrepancy between both CDFs within the first few hundred au, illustrates the lack of close companions found in this study, based on the Gaia direct imaging detection performance.

of close companions is evident in an increasing discrepancy of the CDFs within the first few hundred au. Beyond about 600 au, the discrepancy decreases in agreement with the Gaia detection limit, which allows the detection of even low-mass companions down to $0.1 M_{\odot}$ in this range of projected separation. This highlights the need of high contrast adaptive optics and lucky-imaging surveys to detect missing close companions of the targets, such as those carried out, for example, by Lillo-Box et al. (2024), or Matson et al. (2025) specifically for TOIs, or for exoplanet host stars in general, for example, by

⁹Online available at: https://www.astro.gsu.edu/wds/Supplement/wdss_summ.txt.

Ginski, Mugrauer, Adam, Vogt, and van Holstein (2021), or Schlagenhauf et al. (2024).

The companions found in this study have masses of about 0.12 to 1.6 M_{\odot} and are most frequent in the mass range up to 0.6 M_{\odot} . In addition to low-mass main sequence stars (mainly mid-M to late-K dwarfs), five white dwarfs are identified in this study as companions of (C)TOIs, whose true nature is unveiled by their photometric properties.

For 72 (i.e., 75 % of all) companions presented here, a significant ($\text{sig-}\mu_{\text{rel}} \geq 3$) differential proper motion μ_{rel} relative to the associated (C)TOIs is detected. Using the approximation described in Mugrauer (2019), we derive the escape velocity μ_{esc} of all these companions. The differential proper motion of the majority of these companions is in agreement with orbital motion. In contrast, the differential proper motion of 9 companions significantly exceeds the expected escape velocity. Because these companions all have a high degree of common proper motion ($\text{cpm-index} \geq 12$), this could indicate a higher degree of multiplicity as described in Mugrauer (2019). Follow-up (high contrast imaging) observations are required to further investigate the multiplicity status of all these particular systems and their companions, which are summarized in Table 2.

TABLE 2 In this table we list all detected companions (sorted by their identifier) whose differential proper motion μ_{rel} relative to the associated (C)TOIs significantly exceeds the expected escape velocity μ_{esc} .

Companion	μ_{rel} [mas/yr]	μ_{esc} [mas/yr]
TOI 5122 B	6.43 ± 0.22	2.55 ± 0.01
TOI 5285 A	3.85 ± 0.23	1.82 ± 0.01
TOI 5540 B	2.17 ± 0.05	1.93 ± 0.02
TOI 5544 B	5.48 ± 0.20	4.85 ± 0.05
TOI 5606 A	1.54 ± 0.02	0.70 ± 0.01
CTOI 51099561 B	4.82 ± 0.06	4.37 ± 0.02
CTOI 246976997 B	6.28 ± 0.05	3.08 ± 0.02
CTOI 257554718 B	2.31 ± 0.29	0.99 ± 0.01
CTOI 376973804 B	12.43 ± 0.09	7.34 ± 0.05

The survey, the latest results of which are presented in this paper, is an ongoing project whose target list is continuously growing due to the increasing number of potential exoplanet host stars identified by the TESS mission. In the course of our survey, the multiplicity status of several thousand (C)TOIs has already been investigated, and all these targets are listed in Table S1, which is available online as Supporting Information

Material to this article. The properties of the detected stellar companions of the targets of this survey are regularly reported in this journal, online in the VizieR database, and on the website of the survey¹⁰. The results of our survey, in combination with those of ongoing high-contrast imaging observations of (C)TOIs, which can detect close companions at projected separations down to only a few au, will complete our knowledge of the multiplicity of all these potential exoplanet host stars.

5 | SUPPORTING INFORMATION

Table S1: This tab-separated table contains for all targets, whose multiplicity has been studied in the course of this survey so far, their TIC identifier, and J2000 equatorial coordinates, as listed in the TESS Input Catalog (TIC version 8.2, Paegert et al., 2021), which is online available in the VizieR database.

REFERENCES

- Anders, F., Khalatyan, A., Chiappini, C. et al. (2019, August), *A&A*, 628, A94.
- Anders, F., Khalatyan, A., Queiroz, A. B. A. et al. (2022, February), *A&A*, 658, A91.
- Bédard, A., Bergeron, P., Brassard, P., & Fontaine, G. (2020, October), *ApJ*, 901(2), 93.
- Bergeron, P., Wesemael, F., Dufour, P. et al. (2011, August), *ApJ*, 737(1), 28.
- Blouin, S., Dufour, P., & Allard, N. F. (2018, August), *ApJ*, 863(2), 184.
- El-Badry, K., Rix, H.-W., & Heintz, T. M. (2021, September), *MNRAS*, 506(2), 2269-2295.
- Gaia Collaboration, Brown, A. G. A., Vallenari, A. et al. (2018, August), *A&A*, 616, A1.
- Gaia Collaboration, Brown, A. G. A., Vallenari, A. et al. (2021, May), *A&A*, 649, A1.
- Gaia Collaboration, Vallenari, A., Brown, A. G. A. et al. (2023, June), *A&A*, 674, A1.
- Ginski, C., Mugrauer, M., Adam, C., Vogt, N., & van Holstein, R. G. (2021, May), *A&A*, 649, A156.
- Ginski, C., Mugrauer, M., Seeliger, M. et al. (2016, April), *MNRAS*, 457(2), 2173-2191.
- Holberg, J. B., & Bergeron, P. (2006, September), *AJ*, 132, 1221.
- Kervella, P., Arenou, F., & Thévenin, F. (2022, January), *A&A*, 657, A7.
- Kowalski, P. M., & Saumon, D. (2006, November), *ApJL*, 651, L137.
- Lillo-Box, J., Morales-Calderón, M., Barrado, D. et al. (2024, June), *A&A*, 686, A232.
- Mason, B. D., Wycoff, G. L., Hartkopf, W. I., Douglass, G. G., & Worley, C. E. (2001, December), *AJ*, 122(6), 3466-3471.
- Matson, R. A., Gore, R., Howell, S. B. et al. (2025, February), *AJ*, 169(2), 76.
- Michel, K.-U., & Mugrauer, M. (2024, January), *MNRAS*, 527(2), 3183-3195.

¹⁰Online available at: [https://www.astro.uni-jena.de/Users/markus/Multiplicity_of_\(C\)TOIs.html](https://www.astro.uni-jena.de/Users/markus/Multiplicity_of_(C)TOIs.html).

- Mugrauer, M. (2016, March), *Astronomische Nachrichten*, 337(3), 226-234.
- Mugrauer, M. (2019, December), *MNRAS*, 490(4), 5088.
- Mugrauer, M., & Ginski, C. (2015, July), *MNRAS*, 450(3), 3127-3136.
- Mugrauer, M., Ginski, C., & Seeliger, M. (2014, March), *MNRAS*, 439(1), 1063-1070.
- Mugrauer, M., & Michel, K.-U. (2020, December), *Astronomische Nachrichten*, 341(10), 996-1030.
- Mugrauer, M., & Michel, K.-U. (2021, July), *Astronomische Nachrichten*, 342(6), 840-864.
- Mugrauer, M., Rück, J., & Michel, K. U. (2023, September), *Astronomische Nachrichten*, 344(7), e20230055.
- Mugrauer, M., Zander, J., & Michel, K.-U. (2022, July), *Astronomische Nachrichten*, 343, e24017.
- Paegert, M., Stassun, K. G., Collins, K. A. et al. (2021, August), *arXiv e-prints*, arXiv:2108.04778.
- Pecaut, M. J., & Mamajek, E. E. (2013, September), *ApJS*, 208, 9.
- Raghavan, D., McAlister, H. A., Henry, T. J. et al. (2010, September), *ApJS*, 190(1), 1-42.
- Ricker, G. R., Winn, J. N., Vanderspek, R. et al. (2015, January), *JATIS*, 1, 014003.
- Schlafly, E. F., & Finkbeiner, D. P. (2011, August), *ApJ*, 737(2), 103.
- Schlagenhauf, S., Mugrauer, M., Ginski, C., Buder, S., Fernández, M., & Bischoff, R. (2024, April), *MNRAS*, 529(4), 4768-4786.
- Schlegel, D. J., Finkbeiner, D. P., & Davis, M. (1998, June), *ApJ*, 500(2), 525-553.
- Schneider, J., Dedieu, C., Le Sidaner, P., Savalle, R., & Zolotukhin, I. (2011, August), *A&A*, 532, A79.
- Tremblay, P.-E., Bergeron, P., & Gianninas, A. (2011, April), *ApJ*, 730, 128.
- Wang, S., & Chen, X. (2019, June), *ApJ*, 877(2), 116.



ACKNOWLEDGMENTS

We use data from:

- (1) the ESA Gaia mission (<https://www.cosmos.esa.int/gaia>), processed by the Gaia Data Processing and Analysis Consortium (DPAC, <https://www.cosmos.esa.int/web/gaia/dpac/consortium>). The DPAC is funded by national institutions, in particular those participating in the Gaia Multilateral Agreement.
- (2) the Exoplanet Follow-up Observing Program website, operated by the California Institute of Technology, on behalf of the National Aeronautics and Space Administration, under the Exoplanet Exploration Program.
- (3) the Simbad and VizieR databases operated at the CDS in Strasbourg, France.
- (4) the Extrasolar Planets Encyclopaedia.
- (5) the Pan-STARRS1 surveys, made possible by contributions from the Institute for Astronomy, the University of Hawaii, the Pan-STARRS Project Office, the Max-Planck Society and its participating institutes, the Max Planck Institute for Astronomy, Heidelberg and the Max Planck Institute

for Extraterrestrial Physics, Garching, The Johns Hopkins University, Durham University, the University of Edinburgh, the Queen's University Belfast, the Harvard-Smithsonian Center for Astrophysics, the Las Cumbres Observatory Global Telescope Network Incorporated, the National Central University of Taiwan, the Space Telescope Science Institute, and the National Aeronautics and Space Administration under Grant No. NNX08AR22G issued through the Planetary Science Division of the NASA Science Mission Directorate, the National Science Foundation Grant No. AST-1238877, the University of Maryland, Eotvos Lorand University (ELTE), and the Los Alamos National Laboratory. The Pan-STARRS1 Surveys are archived at the Space Telescope Science Institute (STScI) and are available through MAST, the Mikulski Archive for Space Telescopes. Additional support for the Pan-STARRS1 public science archive is provided by the Gordon and Betty Moore Foundation.

(6) the SkyMapper Southern Sky Survey, whose national facility capability has been funded through ARC LIEF grant LE130100104 from the Australian Research Council, awarded to the University of Sydney, the Australian National University, Swinburne University of Technology, the University of Queensland, the University of Western Australia, the University of Melbourne, Curtin University of Technology, Monash University and the Australian Astronomical Observatory. SkyMapper is owned and operated by The Australian National University's Research School of Astronomy and Astrophysics. The survey data were processed and provided by the SkyMapper Team at ANU. The SkyMapper node of the All-Sky Virtual Observatory (ASVO) is hosted at the National Computational Infrastructure (NCI). Development and support of the SkyMapper node of the ASVO has been funded in part by Astronomy Australia Limited (AAL) and the Australian Government through the Commonwealth's Education Investment Fund (EIF) and National Collaborative Research Infrastructure Strategy (NCRIS), particularly the National eResearch Collaboration Tools and Resources (NeCTAR) and the Australian National Data Service Projects (ANDS).

(7) the University Observatory Jena, which is operated by the Astrophysical Institute of the Friedrich-Schiller-University.



TABLE 3 In this table we summarize for all (C)TOIs (listed first, including their TIC identifier) and their detected co-moving companions their Gaia DR3 parallax π , proper motion μ in right ascension and declination, astrometric excess noise $epsi$, G-band magnitude, as well as the used G-Band extinction estimate A_G from the SHC or if not available the G-Band extinction estimate, as listed either in the SHC2 or in the VizieR database, indicated with SHC2, and ✱, respectively.

TOI	TIC	π [mas]	$\mu_\alpha \cos(\delta)$ [mas/yr]	μ_δ [mas/yr]	$epsi$ [mas]	G [mag]	A_G [mag]	
4580 A	219742885	14.7820 ± 0.0092	93.028 ± 0.012	-259.051 ± 0.013	0.044	9.0650 ± 0.0028		
4580 B		14.7760 ± 0.0749	91.284 ± 0.096	-257.824 ± 0.104	0.434	17.4529 ± 0.0029	$0.3114^{+0.3250}_{-0.0277}$	
4601 A	349071261	4.5498 ± 0.0184	4.475 ± 0.020	-14.914 ± 0.015	0.087	10.7645 ± 0.0028		
4601 B		4.5474 ± 0.0265	4.333 ± 0.032	-14.730 ± 0.022	0.015	14.4172 ± 0.0028	$0.1233^{+1.0486}_{-0.0555}$	
4609 A	118820486	2.9102 ± 0.0218	-0.462 ± 0.026	-6.034 ± 0.017	0.109	10.8653 ± 0.0028		
4609 B		2.8447 ± 0.0378	-0.082 ± 0.047	-6.275 ± 0.031	0.232	10.8968 ± 0.0028	$1.1640^{+0.2851}_{-0.2847}$	
4642 B	336961891	42.4443 ± 0.0196	92.003 ± 0.023	-122.038 ± 0.018	0.092	13.2717 ± 0.0028		
4642 A		42.5314 ± 0.0314	94.018 ± 0.035	-120.392 ± 0.026	0.220	12.7336 ± 0.0029	$0.0004^{+0.0154}_{-0.0004}$	✱
4656 A	120523488	2.3036 ± 0.0231	1.995 ± 0.017	-8.516 ± 0.018	0.083	13.9181 ± 0.0028	$0.3610^{+0.1785}_{-0.1480}$	
4656 B		2.2052 ± 0.1509	2.242 ± 0.124	-9.063 ± 0.131	0.300	17.9742 ± 0.0037		
4660 A	435259601	3.8669 ± 0.0198	-2.978 ± 0.024	-27.508 ± 0.018	0.000	14.0977 ± 0.0029		
4660 B		3.6936 ± 0.0848	-3.177 ± 0.096	-27.031 ± 0.078	0.664	14.1363 ± 0.0028	$1.6649^{+0.1333}_{-0.0868}$	
4661 A	441135051	3.6713 ± 0.0429	44.084 ± 0.044	-29.203 ± 0.041	0.294	12.8209 ± 0.0032		
4661 B		3.5748 ± 0.0333	43.829 ± 0.035	-29.113 ± 0.034	0.174	13.0830 ± 0.0028	$0.0000^{+0.9791}_{-0.0000}$	
4668 A	142938659	9.4339 ± 0.0237	35.719 ± 0.021	-4.416 ± 0.028	0.036	15.1633 ± 0.0029		
4668 B		9.4221 ± 0.0256	35.240 ± 0.023	-4.313 ± 0.032	0.109	15.1874 ± 0.0028	$0.0357^{+0.0853}_{-0.0357}$	
4725 A	26587613	2.7530 ± 0.0186	-5.927 ± 0.023	-6.782 ± 0.019	0.097	12.7149 ± 0.0028	$0.1546^{+0.1427}_{-0.1344}$	
4725 B		2.8154 ± 0.0183	-5.882 ± 0.020	-6.747 ± 0.017	0.089	12.7365 ± 0.0029		
4725 C		2.6933 ± 0.4404	-5.353 ± 0.507	-7.231 ± 0.470	0.000	19.7832 ± 0.0060		
4735 A	280292434	5.0151 ± 0.0222	-26.192 ± 0.023	-11.679 ± 0.021	0.131	14.0006 ± 0.0028	$1.3196^{+0.2093}_{-0.1858}$	
4735 B		5.0403 ± 0.0293	-26.315 ± 0.032	-12.548 ± 0.028	0.188	14.6276 ± 0.0029		
4776 A	196286578	2.6684 ± 0.0137	20.123 ± 0.012	-25.989 ± 0.012	0.090	12.0200 ± 0.0028	$0.1915^{+0.1639}_{-0.1692}$	
4776 B		3.0587 ± 0.4433	19.911 ± 0.209	-25.010 ± 0.207	1.053	16.7312 ± 0.0049		
4781 A	176242778	2.0566 ± 0.0200	-5.598 ± 0.020	-3.433 ± 0.017	0.178	12.0275 ± 0.0028		
4781 B		1.8676 ± 0.0299	-5.055 ± 0.030	-3.458 ± 0.024	0.252	12.5995 ± 0.0031	$1.4697^{+0.9211}_{-0.5250}$	
4800 A	280307604	2.7972 ± 0.0595	-4.608 ± 0.061	-0.875 ± 0.050	0.358	11.3544 ± 0.0028		
4800 B		2.4874 ± 0.0403	-4.454 ± 0.043	-0.196 ± 0.034	0.242	12.4439 ± 0.0028	$0.2717^{+0.1543}_{-0.1270}$	
4858 A	262499797	5.0381 ± 0.0331	54.190 ± 0.051	-92.530 ± 0.037	0.000	16.0502 ± 0.0029	$1.3313^{+0.2620}_{-0.4418}$	✱
4858 B		4.4085 ± 0.5066	51.909 ± 0.838	-93.231 ± 0.611	2.174	20.0915 ± 0.0065		
4944 A	242190195	2.0978 ± 0.0190	6.390 ± 0.017	-22.878 ± 0.023	0.000	13.4861 ± 0.0028	$0.2996^{+0.1343}_{-0.1891}$	
4944 B		1.1986 ± 0.2024	6.235 ± 0.190	-21.967 ± 0.289	1.154	16.7061 ± 0.0037		
4980 A	200435203	1.5847 ± 0.2332	-2.801 ± 0.260	1.209 ± 0.285	2.650	13.4775 ± 0.0031	$0.1345^{+0.2571}_{-0.1345}$	
4980 B		1.2358 ± 0.2898	-2.762 ± 0.327	1.160 ± 0.337	0.939	19.6680 ± 0.0046		
5049 A	261020738	2.0831 ± 0.0148	-5.973 ± 0.008	-7.287 ± 0.014	0.000	13.4514 ± 0.0028		
5049 B		1.5070 ± 0.1882	-6.131 ± 0.096	-6.784 ± 0.181	0.820	17.5603 ± 0.0055	$1.1681^{+1.1354}_{-0.8362}$	
5053 A	324426685	4.6027 ± 0.0119	-10.696 ± 0.011	7.541 ± 0.014	0.039	13.4350 ± 0.0028	$0.5288^{+0.1089}_{-0.1030}$	
5053 B		4.7140 ± 0.4026	-9.869 ± 0.381	7.359 ± 0.420	1.289	20.0350 ± 0.0051		
5069 A	381360757	4.4150 ± 0.0179	7.266 ± 0.019	-42.685 ± 0.015	0.074	10.0745 ± 0.0028		
5069 B		4.2829 ± 0.0559	7.409 ± 0.058	-42.676 ± 0.050	0.000	16.2016 ± 0.0029	$0.6145^{+0.0771}_{-0.0369}$	
5076 A	303432813	12.0845 ± 0.0145	168.778 ± 0.016	-176.012 ± 0.013	0.063	10.5928 ± 0.0028		
5076 B		11.9869 ± 0.0749	168.200 ± 0.077	-175.411 ± 0.065	0.080	16.6446 ± 0.0030	$0.0595^{+0.0126}_{-0.0165}$	
5099 A	91481801	10.8711 ± 0.0352	52.215 ± 0.040	-24.639 ± 0.043	0.137	7.2569 ± 0.0028		
5099 B		10.8657 ± 0.1281	54.508 ± 0.154	-22.473 ± 0.158	0.581	14.2516 ± 0.0043	$0.1870^{+0.0708}_{-0.1258}$	SHC2

TABLE 3 continued

TOI	TIC	π [mas]	$\mu_\alpha \cos(\delta)$ [mas/yr]	μ_δ [mas/yr]	$epsi$ [mas]	G [mag]	A_G [mag]	
5115 A	366499151	4.8429 ± 0.0148	97.723 ± 0.016	-115.749 ± 0.012	0.070	12.6509 ± 0.0028	$0.2213^{+0.1380}_{-0.1293}$	
5115 B		5.1713 ± 0.2641	98.186 ± 0.296	-116.518 ± 0.215	0.475	18.9321 ± 0.0107		
5122 A	116668723	5.5538 ± 0.0205	21.011 ± 0.019	-28.224 ± 0.011	0.087	10.2255 ± 0.0028	$0.3897^{+0.2228}_{-0.2216}$	
5122 B		3.3330 ± 0.2519	26.586 ± 0.243	-31.423 ± 0.143	1.271	14.8256 ± 0.0031		
5128 A	406495245	5.1833 ± 0.0328	-17.336 ± 0.037	-14.671 ± 0.027	0.166	8.4712 ± 0.0028	$0.1927^{+0.1601}_{-0.1724}$	SHC2
5128 B		4.9147 ± 0.0458	-18.252 ± 0.052	-14.385 ± 0.031	0.224	11.0733 ± 0.0030		
5128 C		5.1797 ± 0.1001	-18.281 ± 0.117	-14.065 ± 0.087	0.375	17.0132 ± 0.0029		
5129 A	101520163	4.9568 ± 0.0195	-12.410 ± 0.026	6.692 ± 0.020	0.127	10.5628 ± 0.0028		
5129 B		4.9621 ± 0.1061	-12.933 ± 0.132	7.733 ± 0.113	0.106	17.5724 ± 0.0032	$0.0448^{+0.0183}_{-0.0199}$	
5130 A	75589027	9.9609 ± 0.0218	56.520 ± 0.020	-83.881 ± 0.012	0.089	9.0289 ± 0.0028	$0.1731^{+0.1663}_{-0.1731}$	
5130 B		10.1243 ± 0.1440	55.451 ± 0.146	-83.841 ± 0.081	0.437	16.9184 ± 0.0040		
5148 A	291517604	4.1152 ± 0.0166	9.614 ± 0.012	8.079 ± 0.012	0.085	10.5197 ± 0.0028	$0.3045^{+0.2459}_{-0.2210}$	
5148 B		3.8753 ± 0.2469	9.729 ± 0.277	8.798 ± 0.248	0.823	18.6780 ± 0.0060		
5176 A	437054764	3.7873 ± 0.0369	-71.336 ± 0.042	-27.146 ± 0.033	0.000	15.7132 ± 0.0028	$0.1735^{+0.0360}_{-0.0516}$	
5176 B		4.4470 ± 0.4272	-72.973 ± 0.511	-26.743 ± 0.294	1.170	19.1415 ± 0.0040		
5181 A	346667887	2.1064 ± 0.0139	8.348 ± 0.009	2.698 ± 0.012	0.106	12.2091 ± 0.0028	$0.5724^{+0.1838}_{-0.2059}$	
5181 B		2.3584 ± 0.1212	8.378 ± 0.153	3.626 ± 0.121	0.620	17.2895 ± 0.0034		
5233 A	259100469	4.0102 ± 0.0122	21.392 ± 0.015	87.246 ± 0.015	0.097	11.6274 ± 0.0028		
5233 B		4.0602 ± 0.0224	21.487 ± 0.029	86.729 ± 0.026	0.000	15.3101 ± 0.0028	$0.0765^{+0.0616}_{-0.0379}$	
5241 A	305948428	2.3206 ± 0.0109	-11.861 ± 0.007	-12.065 ± 0.011	0.030	12.6129 ± 0.0028		
5241 B		2.3021 ± 0.0827	-11.787 ± 0.059	-11.742 ± 0.085	0.000	17.7455 ± 0.0029	$0.2793^{+0.0611}_{-0.0998}$	SHC2
5242 A	426122503	2.9992 ± 0.0106	7.698 ± 0.010	-41.388 ± 0.011	0.000	13.3451 ± 0.0028		
5242 B		2.9167 ± 0.0889	7.909 ± 0.093	-41.625 ± 0.093	0.395	17.7388 ± 0.0031	$1.2542^{+0.5444}_{-0.1871}$	
5273 A	172871230	2.2753 ± 0.0105	-8.755 ± 0.012	-17.781 ± 0.012	0.025	12.7128 ± 0.0028		
5273 B		2.2845 ± 0.0980	-8.746 ± 0.112	-17.900 ± 0.116	0.503	17.6242 ± 0.0036	$1.6924^{+0.2772}_{-0.7669}$	
5285 B	250330564	5.3355 ± 0.0191	-52.315 ± 0.019	-82.913 ± 0.018	0.000	13.7481 ± 0.0028		
5285 A		5.5292 ± 0.2424	-49.666 ± 0.234	-80.126 ± 0.223	1.765	12.3317 ± 0.0029	$1.0634^{+0.2244}_{-0.1319}$	
5287 A	909930	2.5977 ± 0.0274	-8.536 ± 0.029	-29.633 ± 0.023	0.160	11.1279 ± 0.0028		
5287 B		2.5694 ± 0.0334	-7.905 ± 0.044	-29.682 ± 0.029	0.170	12.6902 ± 0.0029	$0.0860^{+0.1468}_{-0.0860}$	SHC2
5291 A	250983039	4.6466 ± 0.0969	-4.909 ± 0.103	19.145 ± 0.085	0.665	11.3714 ± 0.0028		
5291 B		4.0770 ± 0.0586	-3.875 ± 0.063	19.634 ± 0.052	0.393	13.1258 ± 0.0029	$0.5832^{+0.1463}_{-0.1195}$	
5292 A	33397739	2.7901 ± 0.0416	-8.733 ± 0.041	-6.862 ± 0.039	0.053	15.8931 ± 0.0029		
5292 B		2.7656 ± 0.1777	-9.300 ± 0.171	-7.163 ± 0.169	0.308	18.4652 ± 0.0036	$0.0893^{+0.0516}_{-0.0151}$	SHC2
5293 A	250111245	6.1645 ± 0.0282	-17.131 ± 0.031	0.487 ± 0.024	0.000	14.9622 ± 0.0028		
5293 B		6.2742 ± 0.1330	-16.497 ± 0.152	-0.079 ± 0.119	0.000	17.8662 ± 0.0034	$0.2981^{+0.0374}_{-0.2981}$	
5294 A	422486295	3.0820 ± 0.0250	12.360 ± 0.034	-11.291 ± 0.022	0.171	12.7674 ± 0.0029	$0.1243^{+0.0625}_{-0.0625}$	✱
5294 B		3.2861 ± 0.0274	12.513 ± 0.031	-10.580 ± 0.023	0.141	12.9076 ± 0.0028		
5296 A	241102583	3.7277 ± 0.0155	44.367 ± 0.016	-7.514 ± 0.017	0.019	13.0509 ± 0.0028		
5296 B		3.7129 ± 0.0181	44.527 ± 0.017	-8.366 ± 0.017	0.000	13.3199 ± 0.0029	$0.6772^{+0.1384}_{-0.1489}$	
5319 A	246965431	16.4500 ± 0.0169	42.116 ± 0.021	-86.609 ± 0.017	0.035	13.1190 ± 0.0029	$0.7196^{+0.0785}_{-0.2637}$	
5319 B		16.2534 ± 0.0480	41.583 ± 0.058	-84.732 ± 0.042	0.252	14.5828 ± 0.0029		
5324 A	408643099	3.5559 ± 0.0185	6.031 ± 0.021	-16.594 ± 0.018	0.000	13.8681 ± 0.0028		
5324 B		3.5616 ± 0.1574	6.482 ± 0.178	-16.680 ± 0.161	0.000	18.2873 ± 0.0034	$0.1844^{+0.0856}_{-0.0676}$	SHC2
5335 A	381360750	3.0155 ± 0.0168	1.682 ± 0.019	-1.920 ± 0.015	0.000	13.0734 ± 0.0028		
5335 B		3.0346 ± 0.0900	1.720 ± 0.093	-1.675 ± 0.081	0.000	17.0253 ± 0.0029	$0.4154^{+0.0389}_{-0.0258}$	

TABLE 3 continued

TOI	TIC	π [mas]	$\mu_\alpha \cos(\delta)$ [mas/yr]	μ_δ [mas/yr]	ϵ [mas]	G [mag]	A_G [mag]	
5337 A	27294830	3.2720 ± 0.0573	12.289 ± 0.065	-15.651 ± 0.051	0.387	13.7008 ± 0.0028		
5337 B		3.3119 ± 0.1361	12.110 ± 0.145	-15.954 ± 0.115	0.472	17.4804 ± 0.0035	$1.2545^{+0.3091}_{-0.2650}$	SHC2
5347 A	21119973	2.9037 ± 0.0227	5.952 ± 0.026	-1.415 ± 0.023	0.062	14.1743 ± 0.0028		
5347 B		2.7994 ± 0.0467	5.662 ± 0.053	-1.598 ± 0.051	0.246	15.0675 ± 0.0030	$0.0005^{+0.1516}_{-0.0005}$	
5385 A	85266608	2.0927 ± 0.0209	-9.210 ± 0.019	0.858 ± 0.019	0.128	11.2328 ± 0.0028		
5385 B		2.3919 ± 0.1228	-8.648 ± 0.120	0.414 ± 0.131	0.228	17.7185 ± 0.0031	$0.1974^{+0.0532}_{-0.0700}$	
5389 A	39143128	5.1298 ± 0.0565	-33.023 ± 0.044	-46.700 ± 0.040	0.098	15.9254 ± 0.0028	$0.0027^{+0.0911}_{-0.0027}$	
5389 B		7.6227 ± 1.2444	-32.538 ± 0.691	-47.623 ± 0.631	0.000	20.1916 ± 0.0067		
5390 A	8853478	5.6819 ± 0.0254	-19.729 ± 0.023	-22.215 ± 0.018	0.121	11.4856 ± 0.0029	$0.3285^{+0.1238}_{-0.1335}$	
5390 B		5.7284 ± 0.1045	-19.446 ± 0.098	-21.749 ± 0.076	0.401	16.5204 ± 0.0035		
5392 A	198512478	20.6143 ± 0.0135	-61.343 ± 0.018	-95.375 ± 0.016	0.099	8.6232 ± 0.0028		
5392 B		20.6001 ± 0.0120	-63.160 ± 0.016	-92.453 ± 0.015	0.089	11.0908 ± 0.0028	$0.0760^{+0.1458}_{-0.0670}$	
5397 A	18019350	7.5004 ± 0.0140	-74.225 ± 0.014	-3.295 ± 0.018	0.074	10.5880 ± 0.0028		
5397 B		7.5385 ± 0.0190	-74.593 ± 0.018	-3.226 ± 0.023	0.127	12.9008 ± 0.0028	$0.0642^{+0.1915}_{-0.0640}$	
5462 A	79971247	3.4434 ± 0.0285	13.507 ± 0.029	-15.233 ± 0.023	0.155	11.2564 ± 0.0028	$0.2253^{+0.1629}_{-0.1391}$	
5462 B		3.2245 ± 0.3854	12.478 ± 0.367	-15.741 ± 0.314	0.915	18.5907 ± 0.0103		
5518 A	386620582	2.3023 ± 0.0235	-6.248 ± 0.022	-15.393 ± 0.017	0.124	11.6631 ± 0.0028		
5518 B		2.3105 ± 0.0226	-6.472 ± 0.021	-15.261 ± 0.016	0.102	12.0640 ± 0.0028	$0.0718^{+0.0953}_{-0.0718}$	SHC2
5530 A	244170332	16.4848 ± 0.0202	241.138 ± 0.021	-192.878 ± 0.016	0.080	12.3423 ± 0.0028	$0.1405^{+0.0394}_{-0.0893}$	
5530 B		16.4699 ± 0.0448	240.601 ± 0.052	-192.594 ± 0.031	0.000	15.2443 ± 0.0028		
5540 A	456305193	4.2720 ± 0.0376	-8.540 ± 0.022	-26.991 ± 0.033	0.331	10.6287 ± 0.0028	$0.2336^{+0.2540}_{-0.2336}$	
5540 B		4.3668 ± 0.0637	-6.892 ± 0.038	-28.406 ± 0.053	0.456	15.1140 ± 0.0030		
5544 A	68893269	8.8661 ± 0.0767	71.459 ± 0.083	-70.534 ± 0.062	0.609	10.9148 ± 0.0028	$0.3246^{+0.1370}_{-0.1587}$	
5544 B		8.6165 ± 0.1255	65.979 ± 0.183	-70.416 ± 0.152	0.497	16.9423 ± 0.0041		
5551 A	387974148	9.9811 ± 0.0152	-26.584 ± 0.018	0.712 ± 0.011	0.000	13.4380 ± 0.0028	$0.1840^{+0.0503}_{-0.0786}$	
5551 B		10.2526 ± 0.1734	-26.815 ± 0.212	0.115 ± 0.134	0.460	18.3372 ± 0.0034		
5567 A	456335739	2.2963 ± 0.0168	-10.549 ± 0.016	-15.827 ± 0.014	0.000	13.8018 ± 0.0028		
5567 B		2.3169 ± 0.0177	-10.504 ± 0.017	-15.825 ± 0.015	0.000	13.9431 ± 0.0028	$0.1687^{+0.1449}_{-0.1276}$	
5578 A	154563411	6.2937 ± 0.0103	-45.050 ± 0.013	-8.363 ± 0.012	0.019	13.0972 ± 0.0028	$0.0764^{+0.1628}_{-0.0764}$	
5578 B		6.2417 ± 0.1382	-45.283 ± 0.176	-7.819 ± 0.162	0.000	18.5988 ± 0.0034		
5606 B	171599496	3.1460 ± 0.0183	7.539 ± 0.017	10.261 ± 0.017	0.000	14.0042 ± 0.0028		
5606 A		3.1284 ± 0.0184	8.918 ± 0.016	10.936 ± 0.015	0.000	13.6769 ± 0.0028	$0.2998^{+0.1518}_{-0.1385}$	
5620 A	165414210	4.5223 ± 0.0142	24.434 ± 0.014	-37.973 ± 0.015	0.059	12.5514 ± 0.0028	$0.3581^{+0.1789}_{-0.1477}$	
5620 B		4.2225 ± 0.1231	24.734 ± 0.138	-37.485 ± 0.158	0.352	17.7859 ± 0.0046		
5626 A	376645976	8.1152 ± 0.0193	-65.474 ± 0.016	-31.153 ± 0.015	0.138	10.2611 ± 0.0028	$0.1223^{+0.1212}_{-0.1179}$	
5626 B		7.9906 ± 0.3347	-65.165 ± 0.325	-31.320 ± 0.252	1.288	19.3796 ± 0.0040		
5628 A	135100529	9.0682 ± 0.0445	-170.769 ± 0.040	-28.445 ± 0.042	0.024	15.5706 ± 0.0028	$0.0695^{+0.0232}_{-0.0356}$	
5628 B		8.9716 ± 0.0974	-170.202 ± 0.094	-28.622 ± 0.088	0.000	17.1961 ± 0.0030		
5630 A	316416562	7.4542 ± 0.0097	17.601 ± 0.010	-46.845 ± 0.013	0.061	10.8306 ± 0.0028	$0.1443^{+0.1281}_{-0.1164}$	
5630 B		7.7131 ± 0.1289	17.686 ± 0.123	-46.811 ± 0.167	0.413	18.5666 ± 0.0033		
5634 A	119585136	3.0895 ± 0.0585	-60.799 ± 0.056	-25.488 ± 0.052	0.000	15.9849 ± 0.0028		
5634 B		2.8990 ± 0.2339	-60.802 ± 0.213	-25.625 ± 0.207	0.274	18.3031 ± 0.0034	$0.0658^{+0.0381}_{-0.0658}$	
5657 A	441736986	3.4188 ± 0.0141	13.655 ± 0.018	-3.616 ± 0.016	0.000	14.0714 ± 0.0028		
5657 B		3.3722 ± 0.0667	13.755 ± 0.084	-3.287 ± 0.071	0.523	16.6299 ± 0.0031	$1.1054^{+0.2620}_{-0.1675}$	
5661 A	349312122	2.3953 ± 0.0140	-0.231 ± 0.016	-8.205 ± 0.015	0.032	13.4637 ± 0.0028		
5661 B		2.2516 ± 0.0962	-0.578 ± 0.111	-8.288 ± 0.099	0.252	17.5767 ± 0.0048	$1.7849^{+0.1846}_{-0.7356}$	

TABLE 3 continued

CTOI=TIC	π [mas]	$\mu_\alpha \cos(\delta)$ [mas/yr]	μ_δ [mas/yr]	ϵ [mas]	G [mag]	A_G [mag]	
29106627 A	7.0234 ± 0.0153	-28.853 ± 0.014	-7.702 ± 0.012	0.067	11.7592 ± 0.0028	$0.0871^{+0.1251}_{-0.0871}$	
29106627 B	6.5615 ± 0.6192	-29.722 ± 0.567	-8.361 ± 0.429	1.068	19.8962 ± 0.0064		
51099561 A	16.4075 ± 0.0640	109.789 ± 0.056	-76.446 ± 0.053	0.523	8.2180 ± 0.0028		
51099561 B	17.0098 ± 0.0305	109.463 ± 0.028	-71.636 ± 0.025	0.226	13.0244 ± 0.0029	$0.0866^{+0.0670}_{-0.0389}$	
73496987 A	8.1130 ± 0.0116	68.141 ± 0.009	-46.748 ± 0.010	0.077	12.1571 ± 0.0028		
73496987 B	8.3217 ± 0.0379	66.663 ± 0.028	-47.595 ± 0.033	0.268	15.4132 ± 0.0028	$0.3337^{+0.0459}_{-0.0519}$	
80435273 A	4.0520 ± 0.0222	12.708 ± 0.025	-7.036 ± 0.018	0.128	11.0797 ± 0.0028	$0.0847^{+0.1778}_{-0.0847}$	
80435273 B	4.0918 ± 0.4537	12.149 ± 0.600	-6.406 ± 0.451	1.314	19.6122 ± 0.0047		
123496379 A	3.9263 ± 0.0111	-13.112 ± 0.014	-31.179 ± 0.012	0.069	11.9313 ± 0.0028		
123496379 B	3.9183 ± 0.0794	-13.270 ± 0.128	-30.782 ± 0.101	0.695	16.1765 ± 0.0031	$0.1616^{+0.1172}_{-0.1496}$	SHC2
125489144 A	6.5278 ± 0.0157	12.826 ± 0.011	35.341 ± 0.011	0.103	12.5269 ± 0.0028	$0.5694^{+0.1248}_{-0.1279}$	
125489144 B	6.3939 ± 0.0867	12.868 ± 0.062	36.723 ± 0.081	0.434	16.8067 ± 0.0029		
130718055 A	13.0123 ± 0.0238	35.782 ± 0.026	-15.263 ± 0.012	0.106	10.1216 ± 0.0028		
130718055 B	13.0071 ± 0.0272	34.887 ± 0.031	-15.089 ± 0.017	0.078	14.4251 ± 0.0029	$0.0506^{+0.0189}_{-0.0506}$	
154927164 A	5.2602 ± 0.0367	-51.116 ± 0.053	-19.599 ± 0.044	0.139	16.3528 ± 0.0030	$0.3115^{+0.0489}_{-0.0279}$	
154927164 B	5.4197 ± 0.1136	-51.390 ± 0.174	-19.556 ± 0.134	0.458	18.4543 ± 0.0033		
178143624 A	5.3204 ± 0.0232	-9.289 ± 0.026	-18.950 ± 0.021	0.165	11.5675 ± 0.0028		
178143624 B	5.2906 ± 0.0319	-8.991 ± 0.035	-18.721 ± 0.030	0.105	14.7117 ± 0.0028	$0.2521^{+0.0489}_{-0.0350}$	
199660056 A	6.2238 ± 0.0126	-31.712 ± 0.014	-49.181 ± 0.017	0.080	11.6897 ± 0.0028	$0.0976^{+0.1202}_{-0.0976}$	
199660056 B	6.1721 ± 0.1345	-31.926 ± 0.142	-48.341 ± 0.175	0.543	18.0681 ± 0.0040		
237204346 A	3.4136 ± 0.0120	19.232 ± 0.016	30.312 ± 0.015	0.099	11.0394 ± 0.0028	$0.1474^{+0.2028}_{-0.1474}$	
237204346 B	3.6087 ± 0.1718	19.353 ± 0.247	30.544 ± 0.202	0.801	18.8487 ± 0.0055		
241249530 A	2.9570 ± 0.0153	7.620 ± 0.018	-15.717 ± 0.015	0.101	11.5593 ± 0.0028	$0.3559^{+0.2022}_{-0.1790}$	
241249530 B	3.1728 ± 0.0905	7.766 ± 0.107	-15.799 ± 0.092	0.125	17.4606 ± 0.0040		
246976997 A	11.8090 ± 0.0538	41.975 ± 0.064	-110.825 ± 0.051	0.420	12.7758 ± 0.0028		
246976997 B	11.8951 ± 0.0161	41.200 ± 0.021	-104.588 ± 0.017	0.000	13.5784 ± 0.0028	$0.0886^{+0.0520}_{-0.0640}$	
257554718 A	5.2141 ± 0.0192	-4.911 ± 0.019	40.835 ± 0.017	0.118	11.0185 ± 0.0028		
257554718 B	3.5395 ± 0.2891	-2.990 ± 0.290	42.110 ± 0.274	2.254	17.4789 ± 0.0035	$0.2212^{+0.1106}_{-0.0318}$	
199572211 A	14.4304 ± 0.0365	-11.933 ± 0.044	-103.185 ± 0.048	0.406	14.5327 ± 0.0028	$0.4388^{+0.0341}_{-0.0767}$	
199572211 B	14.4517 ± 0.0634	-8.691 ± 0.079	-101.813 ± 0.086	0.621	16.0663 ± 0.0032		
287643871 A	4.7152 ± 0.0209	23.466 ± 0.013	-32.590 ± 0.016	0.149	10.0678 ± 0.0028	$0.4076^{+0.2319}_{-0.3951}$	
287643871 B	5.0993 ± 0.0908	22.196 ± 0.068	-36.095 ± 0.126	0.353			
320261550 A	2.6690 ± 0.0885	15.015 ± 0.066	-50.948 ± 0.070	0.745	11.6670 ± 0.0028	$0.2429^{+0.1791}_{-0.1167}$	
320261550 B	3.0603 ± 0.2235	14.643 ± 0.179	-49.992 ± 0.190	0.429	18.8900 ± 0.0035		
333792947 A	6.7063 ± 0.0181	-51.995 ± 0.017	-50.514 ± 0.013	0.098	10.6233 ± 0.0028	$0.0673^{+0.1337}_{-0.0673}$	
333792947 B	6.8644 ± 0.6154	-51.334 ± 0.842	-51.407 ± 0.489	1.546	20.2015 ± 0.0064		
336892053 A	5.0249 ± 0.0218	26.890 ± 0.026	-12.772 ± 0.019	0.137	11.4605 ± 0.0028	$0.0862^{+0.1418}_{-0.0862}$	
336892053 B	4.7220 ± 0.4689	27.186 ± 0.556	-13.132 ± 0.379	1.909	19.5777 ± 0.0046		
355640518 A	4.3590 ± 0.0383	7.527 ± 0.050	-41.367 ± 0.041	0.088	15.5950 ± 0.0029		
355640518 B	4.1693 ± 0.0912	9.297 ± 0.117	-41.767 ± 0.101	0.295	16.9860 ± 0.0029	$0.2089^{+0.0287}_{-0.0233}$	
359046756 A	6.4011 ± 0.0238	-9.236 ± 0.018	-23.787 ± 0.022	0.202	11.7817 ± 0.0028	$0.2898^{+0.1307}_{-0.1102}$	
359046756 B	6.2385 ± 0.2553	-10.245 ± 0.180	-24.988 ± 0.208	0.920	18.9581 ± 0.0074		
376457352 B	8.4273 ± 0.0258	42.314 ± 0.028	39.584 ± 0.022	0.150	10.4927 ± 0.0028		
376457352 A	8.4022 ± 0.0156	42.280 ± 0.019	39.894 ± 0.014	0.053	9.2576 ± 0.0028	$0.0044^{+0.1874}_{-0.0044}$	
376973804 A	12.9222 ± 0.0766	23.591 ± 0.091	147.484 ± 0.091	0.876	10.2497 ± 0.0028	$0.4544^{+0.1616}_{-0.1821}$	
376973804 B	12.3639 ± 0.0160	34.787 ± 0.018	152.890 ± 0.020	0.143	11.9360 ± 0.0028		
379376771 A	3.4568 ± 0.0149	7.305 ± 0.013	-2.240 ± 0.016	0.000	14.1406 ± 0.0030	$0.4784^{+0.2691}_{-0.0430}$	SHC2
379376771 B	2.2507 ± 0.6848	7.890 ± 0.742	-3.441 ± 0.846	1.793	20.5039 ± 0.0072		

TABLE 3 continued

CTOI=TIC	π [mas]	$\mu_\alpha \cos(\delta)$ [mas/yr]	μ_δ [mas/yr]	$epsi$ [mas]	G [mag]	A_G [mag]	
388076422 B	8.5120 ± 0.0163	-2.430 ± 0.020	-5.109 ± 0.021	0.000	14.2959 ± 0.0028		
388076422 A	8.5280 ± 0.0135	-2.238 ± 0.016	-5.556 ± 0.017	0.096	9.5818 ± 0.0028	$0.0827^{+0.1591}_{-0.0827}$	
389041242 A	4.6607 ± 0.0235	-20.289 ± 0.022	-8.591 ± 0.013	0.081	9.4602 ± 0.0028	$0.3500^{+0.3226}_{-0.2975}$	
389041242 B	3.7849 ± 0.1270	-21.288 ± 0.122	-8.247 ± 0.071	0.619	15.3608 ± 0.0030		
415732733 A	2.5769 ± 0.0179	9.245 ± 0.017	-12.775 ± 0.018	0.148	11.2274 ± 0.0028		
415732733 B	2.5354 ± 0.0172	9.723 ± 0.016	-12.393 ± 0.016	0.130	11.6734 ± 0.0028	$0.1052^{+0.1107}_{-0.1052}$	SHC2
446044800 A	3.8032 ± 0.0225	10.967 ± 0.031	-6.842 ± 0.021	0.132	13.0133 ± 0.0028	$2.9435^{+0.4187}_{-0.1107}$	SHC2
446044800 B	4.0823 ± 0.5194	11.482 ± 0.721	-7.463 ± 0.478	2.895	19.3764 ± 0.0122		

TABLE 4 In this table we list for each detected companion (sorted by its identifier) the angular separation ρ and position angle PA to the associated (C)TOI, the difference between its parallax and that of the (C)TOI $\Delta\pi$ with its significance (in brackets calculated also by taking into account the Gaia astrometric excess noise), the differential proper motion μ_{rel} of the companion relative to the (C)TOI with its significance, as well as its *cpm-index*. The last column indicates if the detected companion is not listed in the WDS (★) and WDSS (★★) as companion(-candidate) of the (C)TOI.

TOI	ρ [arcsec]	PA [°]	$\Delta\pi$ [mas]	$\text{sig-}\Delta\pi$	μ_{rel} [mas/yr]	$\text{sig-}\mu_{\text{rel}}$	<i>cpm-index</i>	not in WDS(S)
4580 B	28.83923 ± 0.00008	147.04551 ± 0.00015	0.01 ± 0.08	0.1 (0.0)	2.13 ± 0.10	21.4	257	
4601 B	13.50476 ± 0.00002	37.30170 ± 0.00010	0.00 ± 0.03	0.1 (0.0)	0.23 ± 0.03	7.4	133	★
4609 B	22.37831 ± 0.00003	322.91646 ± 0.00008	0.07 ± 0.04	1.5 (0.3)	0.45 ± 0.05	9.2	27	★
4642 A	110.76534 ± 0.00003	238.42220 ± 0.00002	0.09 ± 0.04	2.4 (0.4)	2.60 ± 0.04	68.3	117	
4656 B	1.82101 ± 0.00011	324.92595 ± 0.00355	0.10 ± 0.15	0.6 (0.3)	0.60 ± 0.13	4.6	30	★
4660 B	5.68704 ± 0.00007	345.72785 ± 0.00076	0.17 ± 0.09	2.0 (0.3)	0.52 ± 0.08	6.2	106	★
4661 B	0.97469 ± 0.00004	67.26731 ± 0.00251	0.10 ± 0.05	1.8 (0.3)	0.27 ± 0.06	4.8	390	★
4668 B	20.91123 ± 0.00003	194.94794 ± 0.00007	0.01 ± 0.03	0.3 (0.1)	0.49 ± 0.03	15.4	146	★
4725 B	3.47521 ± 0.00002	333.51156 ± 0.00038	0.06 ± 0.03	2.4 (0.5)	0.06 ± 0.03	2.0	315	★
4725 C	20.21887 ± 0.00036	285.89303 ± 0.00096	0.06 ± 0.44	0.1 (0.1)	0.73 ± 0.49	1.5	25	★★
4735 B	1.83179 ± 0.00003	352.79459 ± 0.00099	0.03 ± 0.04	0.7 (0.1)	0.88 ± 0.04	25.0	66	★
4776 B	1.22640 ± 0.00026	105.69781 ± 0.01939	0.39 ± 0.44	0.9 (0.3)	1.00 ± 0.21	4.8	65	★
4781 B	1.28545 ± 0.00002	358.63232 ± 0.00124	0.19 ± 0.04	5.3 (0.6)	0.54 ± 0.04	15.1	23	★
4800 B	6.13520 ± 0.00005	9.71246 ± 0.00055	0.31 ± 0.07	4.3 (0.7)	0.70 ± 0.06	11.4	13	
4858 B	36.33844 ± 0.00051	35.89644 ± 0.00079	0.63 ± 0.51	1.2 (0.3)	2.39 ± 0.82	2.9	90	★
4944 B	2.24130 ± 0.00017	75.89413 ± 0.00438	0.90 ± 0.20	4.4 (0.8)	0.92 ± 0.29	3.2	50	★
4980 B	14.86605 ± 0.00035	41.35600 ± 0.00133	0.35 ± 0.37	0.9 (0.1)	0.06 ± 0.43	0.1	97	★★
5049 B	1.68305 ± 0.00014	214.33608 ± 0.00390	0.58 ± 0.19	3.1 (0.7)	0.53 ± 0.18	3.0	35	★★
5053 B	7.72716 ± 0.00036	196.67239 ± 0.00225	0.11 ± 0.40	0.3 (0.1)	0.85 ± 0.38	2.2	30	★
5069 B	26.27029 ± 0.00005	258.30703 ± 0.00010	0.13 ± 0.06	2.3 (1.4)	0.14 ± 0.06	2.3	604	★
5076 B	26.00300 ± 0.00006	330.04099 ± 0.00014	0.10 ± 0.08	1.3 (0.8)	0.83 ± 0.07	11.5	584	
5099 B	3.17353 ± 0.00013	56.36330 ± 0.00242	0.01 ± 0.13	0.0 (0.0)	3.15 ± 0.16	19.6	37	★
5115 B	3.40570 ± 0.00023	93.42056 ± 0.00264	0.33 ± 0.26	1.2 (0.6)	0.90 ± 0.24	3.7	339	★
5122 B	3.64290 ± 0.00018	50.55511 ± 0.00265	2.22 ± 0.25	8.8 (1.7)	6.43 ± 0.22	28.8	12	★★
5128 B	1.46947 ± 0.00004	356.95198 ± 0.00211	0.27 ± 0.06	4.8 (0.9)	0.96 ± 0.06	15.4	48	
5128 C	29.43633 ± 0.00009	31.95409 ± 0.00018	0.00 ± 0.11	0.0 (0.0)	1.12 ± 0.11	9.8	41	★
5129 B	12.54948 ± 0.00010	282.23270 ± 0.00045	0.01 ± 0.11	0.0 (0.0)	1.16 ± 0.12	9.8	25	★
5130 B	5.89943 ± 0.00008	343.33835 ± 0.00112	0.16 ± 0.15	1.1 (0.3)	1.07 ± 0.15	7.3	189	★
5148 B	4.81438 ± 0.00017	290.75719 ± 0.00182	0.24 ± 0.25	1.0 (0.3)	0.73 ± 0.25	2.9	35	★
5176 B	1.96225 ± 0.00024	328.45046 ± 0.00857	0.66 ± 0.43	1.5 (0.5)	1.69 ± 0.50	3.4	91	★
5181 B	1.65364 ± 0.00010	172.47774 ± 0.00386	0.25 ± 0.12	2.1 (0.4)	0.93 ± 0.12	7.6	19	★
5233 B	10.82636 ± 0.00002	24.42815 ± 0.00013	0.05 ± 0.03	2.0 (0.5)	0.53 ± 0.03	17.5	341	
5241 B	7.24523 ± 0.00005	230.81927 ± 0.00045	0.02 ± 0.08	0.2 (0.2)	0.33 ± 0.08	3.9	101	★
5242 B	3.49198 ± 0.00007	89.09553 ± 0.00123	0.08 ± 0.09	0.9 (0.2)	0.32 ± 0.09	3.4	266	★
5273 B	3.46950 ± 0.00009	197.39491 ± 0.00144	0.01 ± 0.10	0.1 (0.0)	0.12 ± 0.12	1.0	333	★
5285 A	5.80929 ± 0.00019	42.12495 ± 0.00192	0.19 ± 0.24	0.8 (0.1)	3.85 ± 0.23	16.8	50	★
5287 B	1.58830 ± 0.00004	12.51592 ± 0.00173	0.03 ± 0.04	0.7 (0.1)	0.63 ± 0.05	12.0	97	★
5291 B	6.44139 ± 0.00009	359.71348 ± 0.00091	0.57 ± 0.11	5.0 (0.7)	1.14 ± 0.12	9.8	35	
5292 B	9.42981 ± 0.00016	51.57081 ± 0.00095	0.02 ± 0.18	0.1 (0.1)	0.64 ± 0.18	3.7	36	★
5293 B	3.57016 ± 0.00012	79.26403 ± 0.00164	0.11 ± 0.14	0.8 (0.8)	0.85 ± 0.14	6.0	40	★
5294 B	1.21682 ± 0.00003	308.05059 ± 0.00141	0.20 ± 0.04	5.5 (0.9)	0.73 ± 0.03	22.3	46	★
5296 B	4.92901 ± 0.00002	130.99644 ± 0.00024	0.01 ± 0.02	0.6 (0.5)	0.87 ± 0.02	36.1	104	★

TABLE 4 continued

TOI	ρ [arcsec]	PA [°]	$\Delta\pi$ [mas]	sig - $\Delta\pi$	μ_{rel} [mas/yr]	sig - μ_{rel}	cpm - $index$	not in WDS(S)
5319 B	3.03736 ± 0.00004	205.52996 ± 0.00080	0.20 ± 0.05	3.9 (0.8)	1.95 ± 0.05	41.8	98	★
5324 B	5.89184 ± 0.00013	175.53782 ± 0.00145	0.01 ± 0.16	0.0 (0.0)	0.46 ± 0.18	2.6	77	★
5335 B	5.76672 ± 0.00007	277.59977 ± 0.00065	0.02 ± 0.09	0.2 (0.2)	0.25 ± 0.08	3.0	20	★
5337 B	1.96436 ± 0.00009	180.78058 ± 0.00369	0.04 ± 0.15	0.3 (0.1)	0.35 ± 0.14	2.6	113	★
5347 B	1.99340 ± 0.00004	120.99555 ± 0.00122	0.10 ± 0.05	2.0 (0.4)	0.34 ± 0.06	5.9	35	★
5385 B	6.69990 ± 0.00012	172.76240 ± 0.00088	0.30 ± 0.12	2.4 (1.0)	0.72 ± 0.13	5.7	25	★
5389 B	12.55341 ± 0.00085	335.79706 ± 0.00254	2.49 ± 1.25	2.0 (2.0)	1.04 ± 0.65	1.6	110	★
5390 B	2.53375 ± 0.00007	201.00858 ± 0.00195	0.05 ± 0.11	0.4 (0.1)	0.55 ± 0.08	6.4	108	★
5392 B	11.47138 ± 0.00002	155.49563 ± 0.00010	0.01 ± 0.02	0.8 (0.1)	3.44 ± 0.02	152.6	65	
5397 B	26.05021 ± 0.00002	92.51147 ± 0.00005	0.04 ± 0.02	1.6 (0.3)	0.37 ± 0.02	16.2	398	
5462 B	4.45576 ± 0.00032	293.35550 ± 0.00410	0.22 ± 0.39	0.6 (0.2)	1.15 ± 0.36	3.2	35	★
5518 B	2.58880 ± 0.00002	320.10931 ± 0.00052	0.01 ± 0.03	0.3 (0.1)	0.26 ± 0.03	9.0	128	★
5530 B	11.07450 ± 0.00003	26.67810 ± 0.00021	0.01 ± 0.05	0.3 (0.2)	0.61 ± 0.05	11.6	1016	
5540 B	2.80797 ± 0.00005	209.63715 ± 0.00076	0.09 ± 0.07	1.3 (0.2)	2.17 ± 0.05	41.3	26	★
5544 B	2.49444 ± 0.00010	178.70509 ± 0.00322	0.25 ± 0.15	1.7 (0.3)	5.48 ± 0.20	27.3	36	★
5551 B	37.16531 ± 0.00015	235.64238 ± 0.00021	0.27 ± 0.17	1.6 (0.6)	0.64 ± 0.15	4.4	83	★
5567 B	8.04728 ± 0.00002	13.06587 ± 0.00013	0.02 ± 0.02	0.8 (0.8)	0.05 ± 0.02	1.9	844	★
5578 B	29.88560 ± 0.00012	178.37760 ± 0.00028	0.05 ± 0.14	0.4 (0.4)	0.59 ± 0.16	3.6	155	★
5606 A	7.56543 ± 0.00002	316.50689 ± 0.00016	0.02 ± 0.03	0.7 (0.7)	1.54 ± 0.02	66.1	17	★★
5620 B	3.32727 ± 0.00012	316.19626 ± 0.00210	0.30 ± 0.12	2.4 (0.8)	0.57 ± 0.15	3.7	157	★
5626 B	58.72491 ± 0.00021	150.48596 ± 0.00025	0.12 ± 0.34	0.4 (0.1)	0.35 ± 0.31	1.1	412	★
5628 B	22.65965 ± 0.00008	268.52158 ± 0.00021	0.10 ± 0.11	0.9 (0.9)	0.59 ± 0.10	5.8	582	
5630 B	23.09375 ± 0.00010	119.79307 ± 0.00028	0.26 ± 0.13	2.0 (0.6)	0.09 ± 0.13	0.7	1093	★
5634 B	3.80667 ± 0.00022	187.72980 ± 0.00250	0.19 ± 0.24	0.8 (0.5)	0.14 ± 0.21	0.6	963	★
5657 B	2.19933 ± 0.00007	162.58982 ± 0.00189	0.05 ± 0.07	0.7 (0.1)	0.34 ± 0.07	4.6	82	★
5661 B	2.82858 ± 0.00008	95.81690 ± 0.00162	0.14 ± 0.10	1.5 (0.5)	0.36 ± 0.11	3.2	46	★★

TABLE 4 continued

CTOI	ρ [arcsec]	PA [°]	$\Delta\pi$ [mas]	sig - $\Delta\pi$	μ_{rel} [mas/yr]	sig - μ_{rel}	cpm - $index$	not in WDS(S)
29106627 B	10.37999 ± 0.00043	247.52702 ± 0.00233	0.46 ± 0.62	0.7 (0.4)	1.09 ± 0.52	2.1	56	★
51099561 B	28.08447 ± 0.00006	140.51172 ± 0.00011	0.60 ± 0.07	8.5 (1.0)	4.82 ± 0.06	82.2	55	
73496987 B	4.58833 ± 0.00003	236.88089 ± 0.00034	0.21 ± 0.04	5.3 (0.7)	1.70 ± 0.03	55.4	97	★
80435273 B	5.99073 ± 0.00038	248.53835 ± 0.00308	0.04 ± 0.45	0.1 (0.0)	0.84 ± 0.52	1.6	34	★
123496379 B	1.93228 ± 0.00008	221.65257 ± 0.00233	0.01 ± 0.08	0.1 (0.0)	0.43 ± 0.11	4.0	158	★
125489144 B	2.35644 ± 0.00006	302.51923 ± 0.00144	0.13 ± 0.09	1.5 (0.3)	1.38 ± 0.08	16.9	55	★
130718055 B	81.02682 ± 0.00003	53.97081 ± 0.00002	0.01 ± 0.04	0.1 (0.0)	0.91 ± 0.04	22.8	84	★
154927164 B	34.99119 ± 0.00010	176.98906 ± 0.00021	0.16 ± 0.12	1.3 (0.3)	0.28 ± 0.18	1.5	396	
178143624 B	5.51984 ± 0.00003	116.02747 ± 0.00027	0.03 ± 0.04	0.8 (0.1)	0.38 ± 0.04	9.1	111	★
199572211 B	1.62613 ± 0.00007	330.12105 ± 0.00251	0.02 ± 0.07	0.3 (0.0)	3.52 ± 0.09	38.4	59	★
199660056 B	5.78148 ± 0.00012	1.87768 ± 0.00105	0.05 ± 0.14	0.4 (0.1)	0.87 ± 0.17	5.0	134	★
237204346 B	5.77104 ± 0.00017	167.28659 ± 0.00178	0.20 ± 0.17	1.1 (0.2)	0.26 ± 0.21	1.2	275	★
241249530 B	4.93044 ± 0.00008	204.99356 ± 0.00097	0.22 ± 0.09	2.4 (1.2)	0.17 ± 0.11	1.6	209	★
246976997 B	15.02432 ± 0.00005	48.12895 ± 0.00018	0.09 ± 0.06	1.5 (0.2)	6.28 ± 0.05	116.4	37	
257554718 B	15.75378 ± 0.00022	1.02047 ± 0.00079	1.67 ± 0.29	5.8 (0.7)	2.31 ± 0.29	8.1	36	★
287643871 B	0.80477 ± 0.00010	57.02908 ± 0.00956	0.38 ± 0.09	4.1 (1.0)	3.73 ± 0.12	30.6	22	
320261550 B	12.08541 ± 0.00020	170.15320 ± 0.00084	0.39 ± 0.24	1.6 (0.4)	1.03 ± 0.20	5.1	103	★
333792947 B	19.17506 ± 0.00048	137.05849 ± 0.00148	0.16 ± 0.62	0.3 (0.1)	1.11 ± 0.64	1.7	131	★
336892053 B	18.23203 ± 0.00036	127.74226 ± 0.00103	0.30 ± 0.47	0.6 (0.2)	0.47 ± 0.46	1.0	129	★
355640518 B	2.55404 ± 0.00008	77.63236 ± 0.00151	0.19 ± 0.10	1.9 (0.6)	1.81 ± 0.13	14.4	47	★
359046756 B	6.08946 ± 0.00017	71.40152 ± 0.00162	0.16 ± 0.26	0.6 (0.2)	1.57 ± 0.20	7.9	33	★
376457352 A	80.99367 ± 0.00002	309.73802 ± 0.00001	0.03 ± 0.03	0.8 (0.2)	0.31 ± 0.03	11.9	372	
376973804 B	4.87687 ± 0.00008	62.90705 ± 0.00090	0.56 ± 0.08	7.1 (0.6)	12.43 ± 0.09	133.9	25	
379376771 B	11.53677 ± 0.00053	280.56036 ± 0.00263	1.21 ± 0.68	1.8 (0.6)	1.34 ± 0.83	1.6	12	★★
388076422 A	40.07783 ± 0.00002	327.26457 ± 0.00003	0.02 ± 0.02	0.8 (0.2)	0.49 ± 0.03	18.1	24	★
389041242 B	6.35605 ± 0.00009	297.30798 ± 0.00067	0.88 ± 0.13	6.8 (1.4)	1.06 ± 0.12	8.8	42	★★
415732733 B	2.00504 ± 0.00002	59.95759 ± 0.00063	0.04 ± 0.02	1.7 (0.2)	0.61 ± 0.02	25.9	52	
446044800 B	4.16024 ± 0.00049	80.62962 ± 0.00380	0.28 ± 0.52	0.5 (0.1)	0.81 ± 0.59	1.4	33	★★

TABLE 5 In this table we show the equatorial coordinates (α , δ for epoch 2016.0) of all detected co-moving companions (sorted by their identifier) together with their derived absolute G-band magnitude M_G , projected separation sep , mass, and effective temperature T_{eff} . The flags for all companions, as defined in the text, are listed in the last column of this table.

TOI	α [°]	δ [°]	M_G [mag]	sep [au]	$mass$ [M_\odot]	T_{eff} [K]	Flags
4580 B	242.42571706220	65.82126284363	13.01 ^{+0.03} _{-0.33}	1951	0.14 ^{+0.01} _{-0.01}	2834 ⁺¹⁰⁹ ₋₅	BPRP
4601 B	75.81661135820	24.22625173722	7.14 ^{+0.06} _{-1.05}	2968	0.65 ^{+0.02} _{-0.01}	4418 ⁺¹⁹ ₋₁₅₅	SHC2 BPRP AEN
4609 B	70.37018229541	21.26269129279	2.03 ^{+0.29} _{-0.29}	7690	1.65 ^{+0.18} _{-0.25}	7335 ⁺²⁸³ ₋₈₆₁	SHC2 BPRP AEN
4642 A	30.85827552638	6.79974137729	10.88 ^{+0.01} _{-0.02}	2610	0.30 ^{+0.01} _{-0.01}	3180 ⁺²⁹ ₋₂₈	BPRP AEN
4656 B	2.91065995420	-38.00985393244	10.54 ^{+0.15} _{-0.18}	791	0.30 ^{+0.14} _{-0.11}	3378 ⁺³⁴⁰ ₋₂₈₆	
4660 B	51.99938517259	12.52494179753	5.52 ^{+0.09} _{-0.14}	1471	0.87 ^{+0.07} _{-0.05}	5194 ⁺¹⁷⁷ ₋₁₄₃	BPRP AEN NSS
4661 B	40.52044679463	-17.50163406726	6.16 ^{+0.03} _{-0.98}	265	0.73 ^{+0.20} _{-0.18}	5050 ⁺⁸⁹² ₋₁₀₁₈	
4668 B	52.64552564136	-35.20932766785	10.02 ^{+0.04} _{-0.09}	2217	0.30 ^{+0.06} _{-0.03}	3052 ⁺⁵⁵ ₋₁₂	BPRP AEN
4725 B	108.00844677469	15.34977248291	4.77 ^{+0.14} _{-0.15}	1262	0.93 ^{+0.07} _{-0.08}	5867 ⁺²⁶⁴ ₋₂₉₁	BPRP AEN
4725 C	108.00329177814	15.35044647794	11.83 ^{+0.14} _{-0.15}	7344	0.20 ^{+0.01} _{-0.01}	3135 ⁺¹⁸ ₋₁₇	inter BPRP
4735 B	100.89948849807	-5.55143166603	9.50 ^{+0.19} _{-0.21}	365	0.40 ^{+0.18} _{-0.12}	3572 ⁺⁵⁷⁰ ₋₃₂₅	
4776 B	125.55481160934	-25.06763051147	8.67 ^{+0.17} _{-0.17}	460	0.52 ^{+0.02} _{-0.02}	3703 ⁺⁴⁹ ₋₄₈	inter
4781 B	121.78212444434	-18.72655477400	2.41 ^{+0.53} _{-0.93}	625	1.43 ^{+0.64} _{-0.35}	6521 ⁺³⁵²³ ₋₁₁₆₇	BPRP
4800 B	114.70887523979	4.35804999669	4.17 ^{+0.14} _{-0.17}	2193	0.98 ^{+0.11} _{-0.09}	6102 ⁺³²⁷ ₋₂₅₈	BPRP AEN
4858 B	109.89066528814	-55.72025719269	12.27 ^{+0.45} _{-0.27}	7213	0.17 ^{+0.01} _{-0.02}	3082 ⁺³³ ₋₆₁	inter BPRP
4944 B	210.95261189649	-43.27352661884	8.02 ^{+0.20} _{-0.14}	1068	0.59 ^{+0.01} _{-0.03}	3932 ⁺²⁹ ₋₉₉	inter BPRP
4980 B	70.41543544324	-45.48176870066	10.53 ^{+0.35} _{-0.42}	9381	0.31 ^{+0.05} _{-0.04}	3336 ⁺⁸² ₋₆₈	inter BPRP
5049 B	226.11142327044	-66.20345005275	7.75 ^{+0.84} _{-1.14}	808	0.58 ^{+0.07} _{-0.06}	4133 ⁺²⁵⁷ ₋₂₂₉	SHC2
5053 B	285.66558091709	-77.58455457430	12.82 ^{+0.11} _{-0.11}	1679	0.15 ^{+0.01} _{-0.01}	3007 ⁺¹⁶ ₋₁₆	inter BPRP
5069 B	46.91343005792	15.32319842199	8.72 ^{+0.04} _{-0.08}	5950	0.50 ^{+0.05} _{-0.05}	3557 ⁺⁶⁹ ₋₇₄	BPRP AEN
5076 B	50.50666435934	17.24544286280	11.95 ^{+0.02} _{-0.02}	2152	0.22 ^{+0.01} _{-0.02}	2923 ⁺⁶ ₋₄	BPRP
5099 B	44.79434887878	19.99021854274	10.23 ^{+0.13} _{-0.08}	292	0.33 ^{+0.16} _{-0.13}	3410 ⁺³⁵¹ ₋₂₇₉	
5115 B	127.15546132112	10.24941505705	12.14 ^{+0.13} _{-0.14}	703	0.18 ^{+0.01} _{-0.01}	3098 ⁺¹⁷ ₋₁₆	inter BPRP
5122 B	85.68320979997	30.76355816456	8.16 ^{+0.23} _{-0.23}	656	0.57 ^{+0.03} _{-0.02}	3850 ⁺¹⁰¹ ₋₆₆	inter BPRP
5128 B	143.31761521004	9.16882639535	4.49 ^{+0.18} _{-0.17}	284	1.01 ^{+0.27} _{-0.14}	5588 ⁺⁹⁷⁶ ₋₂₈₂₆	SHC2
5128 C	143.32202070526	9.17535654113	10.66 ^{+0.18} _{-0.17}	5679	0.25 ^{+0.12} _{-0.03}	3014 ⁺⁵² ₋₃₃	BPRP AEN
5129 B	99.69889042928	29.09006190937	11.07 ^{+0.03} _{-0.03}	2532	0.30 ^{+0.02} _{-0.01}	3123 ⁺⁵ ₋₂₁	BPRP AEN
5130 B	85.51589366676	28.24274993609	11.74 ^{+0.18} _{-0.17}	592	0.20 ^{+0.01} _{-0.01}	3146 ⁺²⁰ ₋₂₂	inter BPRP
5148 B	261.23900112910	-58.63258006051	11.45 ^{+0.23} _{-0.25}	1170	0.22 ^{+0.01} _{-0.01}	3181 ⁺³¹ ₋₂₈	inter BPRP
5176 B	135.01919020509	13.27416633022	11.86 ^{+0.06} _{-0.05}	518	0.19 ^{+0.01} _{-0.01}	3132 ⁺⁶ ₋₇	inter
5181 B	280.67753974839	21.69936519062	9.73 ^{+0.21} _{-0.19}	785	0.38 ^{+0.18} _{-0.16}	3532 ⁺⁵²⁷ ₋₃₆₇	
5233 B	291.17630715999	69.12792534863	8.25 ^{+0.04} _{-0.07}	2700	0.60 ^{+0.01} _{-0.01}	3813 ⁺³³ ₋₂₃	BPRP
5241 B	295.48207248825	23.12611920517	9.30 ^{+0.11} _{-0.07}	3122	0.50 ^{+0.04} _{-0.01}	3483 ⁺⁵⁸ ₋₄₆	SHC2 BPRP AEN
5242 B	287.65966543260	35.49570988510	8.86 ^{+0.19} _{-0.55}	1164	0.44 ^{+0.02} _{-0.04}	3957 ⁺³⁰¹ ₋₁₇₈	BPRP AEN
5273 B	299.87847460642	41.74115164172	7.76 ^{+0.77} _{-0.28}	1525	0.55 ^{+0.05} _{-0.04}	4157 ⁺²⁹¹ ₋₃₆₁	BPRP
5285 A	340.97018194418	-1.83736466652	4.85 ^{+0.14} _{-0.23}	1089	0.91 ^{+0.06} _{-0.04}	5481 ⁺³⁴¹ ₋₁₈₇	BPRP AEN
5287 B	328.03878268310	-8.41923684736	4.67 ^{+0.11} _{-0.15}	611	0.94 ^{+0.11} _{-0.12}	5831 ⁺⁷⁸⁰ ₋₂₃₇₈	SHC2
5291 B	338.73321754730	-11.36144610900	5.59 ^{+0.13} _{-0.16}	1386	0.84 ^{+0.05} _{-0.04}	5240 ⁺²²⁹ ₋₁₅₆	BPRP AEN
5292 B	344.22443464007	-8.11812010696	10.70 ^{+0.04} _{-0.07}	3380	0.34 ^{+0.05} _{-0.01}	3187 ⁺⁹ ₋₁	SHC2 BPRP
5293 B	355.82965463346	-2.04490969867	11.43 ^{+0.3} _{-0.04}	579	0.27 ^{+0.01} _{-0.02}	3019 ⁺⁵ ₋₁₃₄	BPRP AEN
5294 B	351.46744366346	4.45510285997	6.03 ^{+0.07} _{-0.07}	395	0.74 ^{+0.21} _{-0.17}	5130 ⁺⁸⁸¹ ₋₁₀₂₆	

TABLE 5 continued

TOI	α [°]	δ [°]	M_G [mag]	sep [au]	$mass$ [M_\odot]	T_{eff} [K]	Flags
5296 B	328.97935135277	-0.93830596959	$5.52^{+0.15}_{-0.14}$	1322	$0.84^{+0.05}_{-0.05}$	5369^{+214}_{-209}	BPRP AEN
5319 B	35.21316612425	23.51966741399	$10.89^{+0.27}_{-0.08}$	185	$0.32^{+0.01}_{-0.01}$	3101^{+4}_{-6}	BPRP
5324 B	35.91130263336	15.48132143882	$10.67^{+0.07}_{-0.09}$	1657	$0.35^{+0.01}_{-0.01}$	3210^{+38}_{-44}	SHC2 BPRP AEN
5335 B	46.95072702962	15.35929469431	$8.82^{+0.03}_{-0.05}$	1912	$0.55^{+0.01}_{-0.05}$	3570^{+53}_{-22}	BPRP AEN
5337 B	77.55608612838	19.63953587476	$10.82^{+0.27}_{-0.32}$	600	$0.25^{+0.14}_{-0.10}$	3280^{+288}_{-294}	
5347 B	36.13723265414	24.10135004532	$7.28^{+0.17}_{-0.16}$	687	$0.70^{+0.01}_{-0.05}$	4179^{+104}_{-201}	BPRP
5385 B	160.63097788008	28.19677946157	$9.26^{+0.08}_{-0.06}$	3202	$0.50^{+0.02}_{-0.05}$	3502^{+58}_{-26}	BPRP AEN
5389 B	168.79981491846	39.36209426242	$13.74^{+0.03}_{-0.10}$	2447			BPRP WD
5390 B	142.44400894727	30.06224781742	$11.08^{+0.14}_{-0.13}$	446	$0.25^{+0.15}_{-0.10}$	3241^{+306}_{-311}	
5392 B	212.62573741757	72.58684434661	$7.57^{+0.07}_{-0.15}$	556	$0.65^{+0.01}_{-0.01}$	4085^{+136}_{-82}	BPRP
5397 B	172.02349593924	39.67232940285	$7.19^{+0.07}_{-0.20}$	3473	$0.70^{+0.01}_{-0.01}$	4271^{+177}_{-107}	BPRP AEN
5462 B	91.09747991820	29.07376227197	$11.05^{+0.15}_{-0.17}$	1294	$0.25^{+0.02}_{-0.02}$	3238^{+30}_{-26}	inter BPRP
5518 B	124.15244115120	16.39297090092	$3.84^{+0.08}_{-0.10}$	1124	$1.07^{+0.11}_{-0.17}$	6306^{+244}_{-162}	SHC2 BPRP AEN
5530 B	6.49077239528	-5.69492423465	$11.46^{+0.09}_{-0.04}$	672	$0.21^{+0.02}_{-0.01}$	3109^{+52}_{-16}	BPRP
5540 B	117.73647336421	67.04252126585	$8.03^{+0.24}_{-0.26}$	657	$0.59^{+0.03}_{-0.03}$	3930^{+54}_{-111}	inter BPRP
5544 B	74.70084177919	18.16834758492	$11.36^{+0.16}_{-0.14}$	281	$0.22^{+0.01}_{-0.01}$	3192^{+17}_{-19}	inter
5551 B	87.11664355630	18.17370176834	$13.15^{+0.08}_{-0.06}$	3724	$0.13^{+0.01}_{-0.01}$	2959^{+9}_{-12}	inter BPRP
5567 B	135.14019040998	49.45367095110	$5.65^{+0.13}_{-0.15}$	3504	$0.83^{+0.03}_{-0.05}$	5223^{+212}_{-175}	BPRP AEN
5578 B	189.26659149982	75.91214058224	$12.52^{+0.08}_{-0.17}$	4748	$0.16^{+0.01}_{-0.01}$	3050^{+22}_{-12}	inter BPRP
5606 A	156.89236585321	22.42776119652	$5.88^{+0.14}_{-0.16}$	2405	$0.79^{+0.02}_{-0.04}$	5162^{+219}_{-182}	BPRP AEN
5620 B	159.70788368198	27.41616709350	$10.70^{+0.15}_{-0.18}$	736	$0.29^{+0.02}_{-0.02}$	3303^{+35}_{-29}	inter BPRP
5626 B	198.30818830247	31.62420359821	$13.80^{+0.12}_{-0.13}$	7236	$0.11^{+0.01}_{-0.01}$	2871^{+17}_{-16}	inter BPRP
5628 B	185.72128171212	18.83653832030	$11.91^{+0.04}_{-0.03}$	2499			BPRP WD
5630 B	236.46116377899	40.37166786062	$12.78^{+0.12}_{-0.13}$	3098	$0.15^{+0.01}_{-0.01}$	3012^{+19}_{-17}	inter BPRP AEN
5634 B	175.64347526468	20.96424081778	$10.41^{+0.08}_{-0.06}$	1232	$0.38^{+0.02}_{-0.05}$	3254^{+31}_{-27}	SHC2 BPRP AEN
5657 B	258.83784456604	76.46840498296	$7.75^{+0.17}_{-0.27}$	643	$0.55^{+0.03}_{-0.04}$	4281^{+274}_{-166}	BPRP
5661 B	222.36941815490	20.61525504777	$7.29^{+0.74}_{-0.19}$	1181	$0.60^{+0.04}_{-0.05}$	4431^{+177}_{-485}	BPRP

TABLE 5 continued

CTOI	α [°]	δ [°]	M_G [mag]	sep [au]	$mass$ [M_\odot]	T_{eff} [K]	Flags
29106627 B	118.32161546570	44.02391278176	14.04 ^{+0.09} _{-0.13}	1478			BPRP WD
51099561 B	108.78812382154	57.27062098263	9.13 ^{+0.04} _{-0.07}	1712	0.53 ^{+0.01} _{-0.03}	3447 ⁺⁵⁹ ₋₂₇	BPRP
73496987 B	154.72975675913	-40.36148352393	9.66 ^{+0.06} _{-0.05}	566	0.48 ^{+0.01} _{-0.14}	3290 ⁺¹⁴ ₋₆₀	BPRP AEN
80435273 B	5.15744205473	28.00127695429	12.57 ^{+0.09} _{-0.18}	1478	0.16 ^{+0.01} _{-0.01}	3043 ⁺²⁵ ₋₁₃	inter BPRP
123496379 B	282.71383958329	45.83846316355	10.06 ^{+0.15} _{-0.12}	492	0.35 ^{+0.15} _{-0.14}	3441 ⁺³⁶⁷ ₋₂₈₈	
125489144 B	354.93318323256	40.59673766213	10.31 ^{+0.13} _{-0.13}	361	0.34 ^{+0.02} _{-0.02}	3379 ⁺²⁵ ₋₂₅	inter BPRP
130718055 B	203.49089405471	-2.22223237509	9.98 ^{+0.06} _{-0.02}	6227	0.40 ^{+0.01} _{-0.01}	3330 ⁺¹¹ ₋₅₂	BPRP
154927164 B	205.60279245879	87.58146256826	11.75 ^{+0.04} _{-0.06}	6652	0.20 ^{+0.01} _{-0.01}	3145 ⁺⁷ ₋₅	inter BPRP AEN
178143624 B	50.13941241190	39.34963790918	8.12 ^{+0.04} _{-0.05}	1037	0.55 ^{+0.01} _{-0.01}	3922 ⁺²⁹ ₋₂₄	BPRP
199572211 B	241.51892772090	60.94859587341	11.95 ^{+0.08} _{-0.04}	113	0.18 ^{+0.09} _{-0.06}	3057 ⁺²⁵¹ ₋₂₉₅	
199660056 B	251.04498228102	56.37254080691	11.94 ^{+0.10} _{-0.13}	929	0.19 ^{+0.01} _{-0.01}	3122 ⁺¹⁶ ₋₁₂	inter BPRP
237204346 B	293.32503811565	76.92013397731	11.37 ^{+0.15} _{-0.21}	1691	0.22 ^{+0.01} _{-0.01}	3191 ⁺²⁸ ₋₁₈	inter BPRP
241249530 B	95.30793309240	53.29377686598	9.46 ^{+0.18} _{-0.21}	1667	0.42 ^{+0.02} _{-0.02}	3520 ⁺⁴⁸ ₋₄₃	inter BPRP
246976997 B	36.02698104174	20.69574023571	8.86 ^{+0.07} _{-0.06}	1272	0.50 ^{+0.01} _{-0.01}	3646 ⁺³¹ ₋₄₈	BPRP AEN
257554718 B	46.32519910846	-21.99770274178	10.48 ^{+0.04} _{-0.12}	3021	0.40 ^{+0.05} _{-0.03}	3174 ⁺⁷¹ ₋₁₁	BPRP
287643871 B	326.83165923610	34.85106117909		171			noGmag
320261550 B	295.26073495396	-54.45474892921	10.78 ^{+0.14} _{-0.20}	4528			BPRP WD
333792947 B	120.18676748700	36.78096025094	14.27 ^{+0.07} _{-0.14}	2859			BPRP WD
336892053 B	17.97484538835	2.62290831567	13.00 ^{+0.09} _{-0.15}	3628	0.14 ^{+0.01} _{-0.01}	2981 ⁺²² ₋₁₃	inter BPRP
355640518 B	79.93016535003	48.13604250820	10.11 ^{+0.04} _{-0.04}	586	0.40 ^{+0.03} _{-0.01}	3272 ⁺⁹ ₋₉	BPRP
359046756 B	182.72407801785	35.75623726018	12.70 ^{+0.12} _{-0.14}	951	0.15 ^{+0.01} _{-0.01}	3024 ⁺²⁰ ₋₁₇	inter BPRP
376457352 A	8.28485614305	7.58589364789	3.87 ^{+0.01} _{-0.19}	9611	1.02 ^{+0.14} _{-0.10}	6120 ⁺³⁸³ ₋₃₂₆	BPRP AEN
376973804 B	284.06813293803	55.60692088124	7.04 ^{+0.19} _{-0.17}	377	0.69 ^{+0.01} _{-0.02}	4293 ⁺¹¹⁸ ₋₆₉	inter BPRP AEN
379376771 B	30.26309237626	68.99613421738	12.72 ^{+0.05} _{-0.27}	3337	0.15 ^{+0.01} _{-0.01}	3021 ⁺³⁹ ₋₇	inter BPRP
388076422 A	317.88377986622	68.41144007368	4.14 ^{+0.09} _{-0.16}	4708	1.05 ^{+0.10} _{-0.10}	6132 ⁺³⁴⁷ ₋₃₃₃	BPRP AEN
389041242 B	142.01983463221	5.81979539158	8.35 ^{+0.30} _{-0.33}	1364	0.55 ^{+0.04} _{-0.03}	3796 ⁺¹³⁶ ₋₈₇	inter BPRP
415732733 B	142.03379819381	78.94502728362	3.63 ^{+0.11} _{-0.12}	778	1.10 ^{+0.15} _{-0.15}	6393 ⁺²⁵⁶ ₋₂₂₆	SHC2 BPRP
446044800 B	71.46590406097	31.83394502732	9.33 ^{+0.12} _{-0.42}	1094	0.44 ^{+0.05} _{-0.01}	3551 ⁺⁸⁷ ₋₂₈	inter BPRP